

Supporting Information

Luminescent Ir(III)-Ln(III) coordination polymers showing slow magnetization relaxation

Kun Fan,^a Song-Song Bao,^a Ran Huo,^a Xin-Da Huang,^a Yu-Jie Liu^a, Zi-Wen Yu,^a Mohamedally Kurmoo,^b and Li-Min Zheng^{*a}

[a] State Key Laboratory of Coordination Chemistry, School of Chemistry and Chemical Engineering, Collaborative Innovation Center of Advanced Microstructures, Nanjing University, Nanjing 210023, P. R. China

[b] Université de Strasbourg, Institut de Chimie, CNRS-UMR7177, 4 rue Blaise Pascal, Strasbourg Cedex 67070, France.

Table of Contents

Table S1. Selected bond lengths [Å] and angles [°] for Ir₂Dy .	S4
Table S2 Selected bond lengths [Å] and angles [°] for Ir₂Er .	S5
Table S3 Hydrogen bonds in Ir₂Er .	S6
Table S4 Selected bond lengths [Å] and angles [°] for Ir₂Yb .	S7
Table S5 Hydrogen bonds in Ir₂Yb .	S8
Table S6 Selected bond lengths [Å] and angles [°] for Ir₄Yb₂ .	S9
Table S7 Hydrogen bonds in Ir₄Yb₂ .	S11
Table S8. Cell parameters of Ir₂Gd and Ir₄Ln₂ .	S12
Table S9. The parameters obtained by Cole-Cole fitting for Ir₂Dy under zero dc field.	S13
Table S10 The parameters obtained by Cole-Cole fitting for Ir₂Dy under 2.0 kOe dc field.	S13
Table S11 The parameters obtained by Cole-Cole fitting for Ir₄Dy₂ under zero dc field.	S13
Table S12 The parameters obtained by Cole-Cole fitting for Ir₄Dy₂ under 2.0 kOe dc field.	S14
Table S13 The parameters obtained by Cole-Cole fitting for Ir₂Er under 1.0 kOe dc field.	S15

Table S14 The parameters obtained by Cole-Cole fitting for Ir₄Er₂ under 1.5 kOe dc field.	S15
Table S15 The parameters obtained by Cole-Cole fitting for Ir₂Yb under 2.0 kOe dc field.	S16
Table S16 The parameters obtained by Cole-Cole fitting for Ir₄Yb₂ under 1.5 kOe dc field.	S16
Figure S1. FT-IR spectra of compounds Ir₂Ln and the free ligand.	S17
Figure S2. FT-IR spectra of compounds Ir₄Ln₂ and the free ligand.	S17
Figure S3. Molecular structure of Ir₂Dy .	S18
Figure S4. Molecular structure of Ir₂Er .	S19
Figure S5. Simulated and experimental powder X-ray diffraction patterns of compounds Ir₂Ln .	S20
Figure S6. Pawley fit of a powder sample of compound Ir₂Gd .	S20
Figure S7. Simulated and experimental powder X-ray diffraction patterns of compounds Ir₄Ln₂ .	S21
Figure S8. Pawley fit of a powder sample of compound Ir₄Gd₂ .	S21
Figure S9. Pawley fit of a powder sample of compound Ir₄Dy₂ .	S22
Figure S10. Pawley fit of a powder sample of compound Ir₄Er₂ .	S22
Figure S11. The χ_M vs. T curves for Ir₂Gd and Ir₄Gd₂ .	S23
Figure S12. The plot of magnetization M vs. H and M vs. H/T at depicted temperatures for Ir₂Ln (Ln=Dy, Er, Yb).	S24
Figure S13. The plot of magnetization M vs. H and M vs. H/T at depicted temperatures for Ir₄Ln₂ (Ln = Dy, Er, Yb).	S25
Figure S14. The in-phase (χ') ac susceptibilities and Cole-Cole plot of Ir₂Dy under zero dc field.	S26
Figure S15. In-phase (χ') and out-of-phase (χ'') ac susceptibilities of Ir₂Dy collected at 1.8 K under dc fields ranging from 0 to 3.0 kOe.	S26
Figure S16. The ac susceptibilities for Ir₂Dy under 2.0 kOe dc field.	S27
Figure S17. The in-phase (χ') ac susceptibilities and Cole-Cole plot of Ir₄Dy₂ under zero dc field.	S27
Figure S18. In-phase (χ') and out-of-phase (χ'') ac susceptibilities of Ir₄Dy₂ collected at 1.8 K under dc fields ranging from 0 to 3.0 kOe.	S28
Figure S19. The ac susceptibility of Ir₄Dy₂ under a 2.0 kOe dc field.	S28
Figure S20. In-phase (χ') and out-of-phase (χ'') ac susceptibilities of Ir₂Er collected at 1.8 K under dc field ranging from 0 to 3.0 kOe.	S29
Figure S21. The ac susceptibilities of Ir₂Er under a 1.0 kOe dc field at different temperatures: (a) frequency dependence of in-phase (χ') and (b) out-of-phase (χ''), (c) Cole-Cole plot and (d) plots of $\ln(\tau)$ vs. $1/T$.	S29

Figure S22. In-phase (χ') and out-of-phase (χ'') ac susceptibilities of Ir₄Er₂ collected at 1.8 K under dc field ranging from 0 to 3.0 kOe.	S30
Figure S23. The ac susceptibilities of Ir₄Er₂ under a 1.5 kOe dc field at different temperatures: (a) frequency dependence of in-phase (χ') and (b) out-of-phase (χ''), (c) Cole-Cole plot and (d) plots of $\ln(\tau)$ vs. 1/T.	S30
Figure S24. In-phase (χ') and out-of-phase ac susceptibility (χ'') of Ir₂Yb collected at 1.8 K under dc fields ranging from 0 to 3.0 kOe.	S31
Figure S25. The in-phase (χ') ac susceptibilities of Ir₂Yb under a 1.0 kOe dc field at different temperatures.	S31
Figure S26. In-phase (χ') and out-of-phase (χ'') ac susceptibilities of Ir₄Yb₂ collected at 1.8 K under dc field ranging from 0 to 3.0 kOe.	S31
Figure S27. The in-phase (χ') ac susceptibilities of Ir₄Yb₂ under a 1.5 kOe dc field at different temperatures.	S32
Figure S28. The absorption spectra of Ir(ppy) ₂ (Hdc bpy) and of compounds Ir₂Ln and Ir₄Ln₂ (Ln = Gd, Dy, Er, Yb) in the solid-state.	S32
Figure S29. The luminescence decay for compounds Ir(ppy) ₂ (Hdc bpy), Ir₂Ln and Ir₄Ln₂ .	S33
Figure S30. Luminescent decay profiles monitored at 975 nm for Ir₂Yb and Ir₄Yb₂ in the solid state at room temperature.	S34
Figure S31. Luminescent decay profiles monitored at 1538 nm for Ir₂Er and Ir₄Er₂ in the solid state at room temperature.	S35
Figure S32. TGA curve of Ir₂Ln and Ir(ppy) ₂ (Hdc bpy).	S36
Figure S33. TGA curve of Ir₄Ln₂ and Ir(ppy) ₂ (Hdc bpy).	S36

Table S1 Selected bond lengths [Å] and angles [°] for **Ir₂Dy**.

Ir1 - N1	2.137(17)	Ir1 - N2	2.157(18)
Ir1 - N3	2.02(2)	Ir1 - N4	2.04(2)
Ir1 - C13	1.998(19)	Ir1 - C24	2.02(2)
Ir2 - N5	2.134(16)	Ir2 - N6	2.106(16)
Ir2 - N7	2.037(19)	Ir2 - N8	2.044(18)
Ir2 - C47	1.97(2)	Ir2 - C58	2.07(2)
Dy1 - O1	2.270(16)	Dy1 - O1W	2.332(19)
Dy1 - O2W	2.384(17)	Dy1 - O3W	2.375(17)
Dy1 - O4W	2.50(2)	Dy1 - O5	2.359(18)
Dy1 - O5W	2.48(3)	Dy1 - O3A	2.376(16)
N1 - Ir1 - N2	76.4(7)	N1 - Ir1 - N3	90.2(7)
N1 - Ir1 - N4	95.1(8)	N1 - Ir1 - C13	96.5(8)
N1 - Ir1 - C24	174.2(9)	N2 - Ir1 - N3	98.1(7)
N2 - Ir1 - N4	85.4(9)	N2 - Ir1 - C13	172.7(8)
N2 - Ir1 - C24	99.6(9)	N3 - Ir1 - N4	174.3(9)
N3 - Ir1 - C13	79.9(8)	N3 - Ir1 - C24	94.6(9)
N4 - Ir1 - C13	97.2(10)	N4 - Ir1 - C24	80.3(10)
C13 - Ir1 - C24	87.6(10)	N5 - Ir2 - N6	76.3(6)
N5 - Ir2 - N7	87.4(7)	N5 - Ir2 - N8	96.8(7)
N5 - Ir2 - C47	97.5(8)	N5 - Ir2 - C58	176.4(8)
N6 - Ir2 - N7	97.1(7)	N6 - Ir2 - N8	88.5(6)
N6 - Ir2 - C47	172.9(8)	N6 - Ir2 - C58	100.8(8)
N7 - Ir2 - N8	173.7(7)	N7 - Ir2 - C47	78.9(8)
N7 - Ir2 - C58	95.1(8)	N8 - Ir2 - C47	95.8(8)
N8 - Ir2 - C58	80.9(8)	C47 - Ir2 - C58	85.5(9)
O1 - Dy1 - O1W	92.8(6)	O1 - Dy1 - O2W	151.1(6)
O1 - Dy1 - O3W	88.8(7)	O1 - Dy1 - O4W	140.1(7)
O1 - Dy1 - O5	85.9(6)	O1 - Dy1 - O5W	73.2(6)
O1 - Dy1 - O3A	79.1(6)	O1W - Dy1 - O2W	89.2(6)
O1W - Dy1 - O3W	142.3(8)	O1W - Dy1 - O4W	78.0(7)
O1W - Dy1 - O5	147.1(7)	O1W - Dy1 - O5W	72.8(7)
O1W - Dy1 - O3A	73.9(6)	O2W - Dy1 - O3W	106.9(7)
O2W - Dy1 - O4W	68.4(7)	O2W - Dy1 - O5	77.1(6)
O2W - Dy1 - O5W	134.4(6)	O2W - Dy1 - O3A	73.8(6)
O3W - Dy1 - O4W	76.8(7)	O3W - Dy1 - O5	70.6(8)
O3W - Dy1 - O5W	71.7(8)	O3A - Dy1 - O3W	142.9(7)
O4W - Dy1 - O5	122.2(7)	O5 - Dy1 - O5W	136.9(7)
O3A - Dy1 - O4W	132.6(7)	O3A - Dy1 - O5W	134.9(7)
O3A - Dy1 - O5	73.6(6)	O4W - Dy1 - O5W	67.0(7)

Symmetry transformations used to generate equivalent atoms: A: -1+x, y, z.

Table S2 Selected bond lengths [Å] and angles [°] for **Ir₂Er**.

Ir1 - N1	2.126(11)	Ir1 - N2	2.159(12)
Ir1 - N3	2.015(11)	Ir1 - N4	2.012(14)
Ir1 - C13	2.008(14)	Ir1 - C24	1.983(17)
Ir2 - N5	2.163(11)	Ir2 - N6	2.149(12)
Ir2 - N7	2.031(11)	Ir2 - N8	2.044(11)
Ir2 - C47	2.000(15)	Ir2 - C58	2.033(14)
Er1 - O1	2.227(11)	Er1 - O1W	2.315(13)
Er1 - O2W	2.28(2)	Er1 - O3W	2.321(11)
Er1 - O4W	2.31(2)	Er1 - O5	2.263(12)
Er1 - O4W'	2.47(3)	Er1 - O3A	2.318(11)
N1 - Ir1 - N2	76.1(5)	N1 - Ir1 - N3	90.0(4)
N1 - Ir1 - N4	96.2(5)	N1 - Ir1 - C13	95.5(5)
N1 - Ir1 - C24	173.4(6)	N2 - Ir1 - N3	98.7(5)
N2 - Ir1 - N4	86.5(5)	N2 - Ir1 - C13	171.5(5)
N2 - Ir1 - C24	98.6(6)	N3 - Ir1 - N4	172.7(5)
N3 - Ir1 - C13	79.9(5)	N3 - Ir1 - C24	94.8(6)
N4 - Ir1 - C13	95.6(6)	N4 - Ir1 - C24	79.3(7)
C13 - Ir1 - C24	89.8(6)	N5 - Ir2 - N6	74.9(4)
N5 - Ir2 - N7	88.2(4)	N5 - Ir2 - N8	95.9(4)
N5 - Ir2 - C47	99.5(5)	N5 - Ir2 - C58	174.9(5)
N6 - Ir2 - N7	95.9(5)	N6 - Ir2 - N8	90.2(5)
N6 - Ir2 - C47	173.4(5)	N6 - Ir2 - C58	102.4(5)
N7 - Ir2 - N8	173.3(5)	N7 - Ir2 - C47	80.3(6)
N7 - Ir2 - C58	96.4(6)	N8 - Ir2 - C47	93.9(6)
N8 - Ir2 - C58	79.7(6)	C47 - Ir2 - C58	83.5(6)
O1 - Er1 - O1W	90.4(5)	O1 - Er1 - O2W	166.7(6)
O1 - Er1 - O3W	82.7(4)	O1 - Er1 - O4W	116.1(7)
O1 - Er1 - O5	94.0(4)	O1 - Er1 - O4W'	78.6(6)
O1 - Er1 - O3A	84.5(4)	O1W - Er1 - O2W	84.4(7)
O1W - Er1 - O3W	136.6(5)	O1W - Er1 - O4W	74.0(8)
O1W - Er1 - O5	148.6(5)	O1W - Er1 - O4W'	67.0(7)
O1W - Er1 - O3A	74.6(4)	O2W - Er1 - O3W	109.4(6)
O2W - Er1 - O4W	74.1(9)	O2W - Er1 - O5	84.4(7)
O2W - Er1 - O4W'	110.2(8)	O2W - Er1 - O3A	82.4(6)
O3W - Er1 - O4W	71.0(7)	O3W - Er1 - O5	74.8(5)
O3W - Er1 - O4W'	69.6(7)	O3A - Er1 - O3W	146.1(4)
O4W - Er1 - O5	130.0(8)	O5 - Er1 - O4W'	144.2(7)
O3A - Er1 - O4W	142.2(7)	O3A - Er1 - O4W'	137.6(7)
O3A - Er1 - O5	75.0(4)		

Symmetry transformations used to generate equivalent atoms: A: -1+x, y, z.

Table S3 Hydrogen bonds in **Ir₂Er**

D-H···A	d(D-H) (Å)	d(H···A) (Å)	d(D···A) (Å)	∠ DHA (°)
O1W-H1WA···O4 ⁱ	0.8500	1.8000	2.578(18)	152.00
O1W-H1WB···O14 ⁱⁱ	0.8600	2.3600	2.95(4)	126.00
O2W-H2WA···O16	0.8500	2.5100	3.16(4)	133.00
O2W-H2WB···O10 ⁱⁱⁱ	0.8500	2.5100	3.16(5)	134.00
O3W-H3WA···O8 ⁱⁱ	0.8500	2.1100	2.801(7)	136.00
O3W-H3WB···O6 ^{iv}	0.8500	1.8300	2.666(17)	166.00
O4W'-H5WA···O14 ⁱⁱ	0.8500	2.4500	3.00(5)	124.00
O4W'-H5WB···O3W	0.8500	2.4300	2.74(3)	102.00
O6W-H6WB···O16	0.8500	2.4900	3.33(10)	173.00
O9-H9A···O11	0.8400	1.9500	2.68(4)	145.00
O10-H10C···O7 ^v	0.8600	1.9900	2.69(3)	138.00

Symmetry transformations used to generate equivalent atoms: i: -1+x, y, z; ii: 1+x, y, z;
iii: 2-x, 1-y, 1-z; iv: 1-x, 2-y, 1-z; v: 2+x, -1+y, z.

Table S4 Selected bond lengths [Å] and angles [°] for **Ir₂Yb**.

Ir1 - N1	2.121(7)	Ir1 - N2	2.151(7)
Ir1 - N3	2.032(7)	Ir1 - N4	2.034(7)
Ir1 - C13	2.001(9)	Ir1 - C24	2.010(9)
Ir2 - N5	2.132(7)	Ir2 - N6	2.119(7)
Ir2 - N7	2.042(7)	Ir2 - N8	2.045(7)
Ir2 - C47	1.996(8)	Ir2 - C58	2.003(7)
Yb1 - O1	2.191(7)	Yb1 - O1W	2.286(7)
Yb1 - O2W	2.253(11)	Yb1 - O3W	2.291(6)
Yb1 - O4W	2.321(10)	Yb1 - O5	2.230(7)
Yb1 - O4W'	2.452(18)	Yb1 - O3A	2.298(6)
N1 - Ir1 - N2	75.3(3)	N1 - Ir1 - N3	89.9(3)
N1 - Ir1 - N4	95.8(3)	N1 - Ir1 - C13	96.6(3)
N1 - Ir1 - C24	174.4(3)	N2 - Ir1 - N3	98.6(3)
N2 - Ir1 - N4	86.4(3)	N2 - Ir1 - C13	171.8(3)
N2 - Ir1 - C24	100.1(3)	N3 - Ir1 - N4	173.2(3)
N3 - Ir1 - C13	80.0(3)	N3 - Ir1 - C24	94.1(3)
N4 - Ir1 - C13	95.7(4)	N4 - Ir1 - C24	80.5(4)
C13 - Ir1 - C24	88.1(4)	N5 - Ir2 - N6	76.3(3)
N5 - Ir2 - N7	88.7(3)	N5 - Ir2 - N8	96.2(3)
N5 - Ir2 - C47	97.4(3)	N5 - Ir2 - C58	174.9(3)
N6 - Ir2 - N7	96.0(3)	N6 - Ir2 - N8	89.5(3)
N6 - Ir2 - C47	172.8(3)	N6 - Ir2 - C58	100.4(3)
N7 - Ir2 - N8	173.4(3)	N7 - Ir2 - C47	80.5(3)
N7 - Ir2 - C58	95.5(3)	N8 - Ir2 - C47	94.4(3)
N8 - Ir2 - C58	79.9(3)	C47 - Ir2 - C58	86.2(3)
O1 - Yb1 - O1W	89.6(2)	O1 - Yb1 - O2W	169.7(3)
O1 - Yb1 - O3W	82.8(2)	O1 - Yb1 - O4W	115.2(3)
O1 - Yb1 - O5	95.0(2)	O1 - Yb1 - O4W'	79.6(5)
O1 - Yb1 - O3A	85.8(2)	O1W - Yb1 - O2W	84.3(4)
O1W - Yb1 - O3W	135.1(3)	O1W - Yb1 - O4W	73.3(3)
O1W - Yb1 - O5	149.8(3)	O1W - Yb1 - O4W'	67.4(5)
O1W - Yb1 - O3A	75.4(2)	O2W - Yb1 - O3W	107.4(3)
O2W - Yb1 - O4W	70.9(4)	O2W - Yb1 - O5	86.3(4)
O2W - Yb1 - O4W'	105.4(5)	O2W - Yb1 - O3A	84.7(3)
O3W - Yb1 - O4W	70.4(3)	O3W - Yb1 - O5	75.1(3)
O3W - Yb1 - O4W'	67.7(5)	O3A - Yb1 - O3W	147.1(2)
O4W - Yb1 - O5	129.7(3)	O5 - Yb1 - O4W'	142.7(5)
O3A - Yb1 - O4W	141.7(3)	O3A - Yb1 - O4W'	139.9(5)
O3A - Yb1 - O5	75.3(2)		

Symmetry transformations used to generate equivalent atoms: A: -1+x, y, z.

Table S5 Hydrogen bonds in **Ir₂Yb**

D-H···A	d(D-H) (Å)	d(H···A) (Å)	d(D···A) (Å)	∠ DHA (°)
O1W-H1WA···O4 ⁱ	0.8500	1.8100	2.600(9)	154.00
O1W-H1WB···O14 ⁱⁱ	0.8600	2.2700	2.857(17)	126.00
O2W-H2WA···O16	0.8500	2.5000	3.16(2)	135.00
O2W-H2WB···O10 ⁱⁱⁱ	0.8500	2.4100	3.07(3)	135.00
O3W-H3WA···O8 ⁱⁱ	0.8500	1.9700	2.649(9)	136.00
O3W-H3WB···O6 ^{iv}	0.8500	1.8300	2.668(10)	167.00
O6W-H6WB···O16	0.8500	2.5800	3.43(4)	174.00
O9-H9A···O11	0.8400	1.9400	2.70(2)	151.00
O10-H10C···O7 ^v	0.8600	1.9600	2.660(14)	138.00

Symmetry transformations used to generate equivalent atoms: i: -1+x, y, z; ii: 1+x, y, z;
iii: 1-x, 1-y, 1-z; iv: 1-x, 2-y, 1-z; v: 1+x, -1+y, z.

Table S6 Selected bond lengths [Å] and angles [°] for **Ir₄Yb₂**.

Ir1 - N1	2.120(15)	Ir1 - N2	2.160(12)
Ir1 - N3	2.029(13)	Ir1 - N4	2.037(12)
Ir1 - C23	2.011(19)	Ir1 - C34	1.999(13)
Ir2 - N5	2.123(12)	Ir2 - N6	2.127(13)
Ir2 - N7	2.036(15)	Ir2 - N8	2.022(15)
Ir2 - C47	2.011(17)	Ir2 - C58	2.002(14)
Ir3 - N9	2.134(13)	Ir3 - N10	2.159(13)
Ir3 - N11	2.030(15)	Ir3 - N12	2.035(15)
Ir3 - C81	2.011(17)	Ir3 - C92	2.023(17)
Ir4 - N13	2.108(15)	Ir4 - N14	2.147(13)
Ir4 - N15	2.026(13)	Ir4 - N16	2.040(16)
Ir4 - C115	2.038(15)	Ir4 - C126	2.01(2)
Yb1 - O1	2.215(9)	Yb1 - O1W	2.367(11)
Yb1 - O2W	2.306(15)	Yb1 - O5	2.190(8)
Yb1 - O9	2.272(11)	Yb1 - O3b	2.366(12)
Yb1 - O28c	2.262(12)	Yb2 - O3W	2.450(11)
Yb2 - O4W	2.329(12)	Yb2 - O11	2.245(12)
Yb2 - O13	2.221(12)	Yb2 - O28	2.205(12)
Yb2 - O7a	2.289(10)	Yb2 - O15b	2.335(12)
N1 - Ir1 - N2	76.1(5)	N1 - Ir1 - N3	94.9(5)
N1 - Ir1 - N4	89.2(5)	N1 - Ir1 - C23	175.0(6)
N1 - Ir1 - C34	95.2(5)	N2 - Ir1 - N3	89.2(5)
N2 - Ir1 - N4	96.9(5)	N2 - Ir1 - C23	101.5(6)
N2 - Ir1 - C34	170.7(5)	N3 - Ir1 - N4	173.3(6)
N3 - Ir1 - C23	80.6(6)	N3 - Ir1 - C34	94.9(5)
N4 - Ir1 - C23	95.4(6)	N4 - Ir1 - C34	79.5(5)
C23 - Ir1 - C34	87.4(6)	N5 - Ir2 - N6	77.0(5)
N5 - Ir2 - N7	89.4(5)	N5 - Ir2 - N8	95.6(6)
N5 - Ir2 - C47	99.5(6)	N5 - Ir2 - C58	172.3(5)
N6 - Ir2 - N7	98.1(5)	N6 - Ir2 - N8	87.0(5)
N6 - Ir2 - C47	175.9(6)	N6 - Ir2 - C58	95.9(5)
N7 - Ir2 - N8	173.5(5)	N7 - Ir2 - C47	79.6(6)
N7 - Ir2 - C58	94.3(6)	N8 - Ir2 - C47	95.4(7)
N8 - Ir2 - C58	81.3(6)	C47 - Ir2 - C58	87.8(6)
N9 - Ir3 - N10	76.8(5)	N9 - Ir3 - N11	87.7(5)
N9 - Ir3 - N12	96.4(5)	N9 - Ir3 - C81	96.4(6)
N9 - Ir3 - C92	175.1(6)	N10 - Ir3 - N11	95.5(6)
N10 - Ir3 - N12	90.7(6)	N10 - Ir3 - C81	172.0(6)
N10 - Ir3 - C92	99.8(6)	N11 - Ir3 - N12	173.2(5)
N11 - Ir3 - C81	80.0(7)	N11 - Ir3 - C92	96.1(7)

N12 - Ir3 - C81	94.2(7)	N12 - Ir3 - C92	80.1(6)
C81 - Ir3 - C92	87.3(7)	N13 - Ir4 - N14	76.2(5)
N13 - Ir4 - N15	89.7(5)	N13 - Ir4 - N16	96.5(6)
N13 - Ir4 - C115	96.3(6)	N13 - Ir4 - C126	174.9(7)
N14 - Ir4 - N15	97.7(5)	N14 - Ir4 - N16	.9(6)
N14 - Ir4 - C115	172.2(6)	N14 - Ir4 - C126	99.4(6)
N15 - Ir4 - N16	173.0(6)	N15 - Ir4 - C115	79.8(6)
N15 - Ir4 - C126	93.4(7)	N16 - Ir4 - C115	96.3(6)
N16 - Ir4 - C126	80.6(7)	C115 - Ir4 - C126	88.2(7)
O1 - Yb1 - O1W	81.4(4)	O1 - Yb1 - O2W	91.4(4)
O1 - Yb1 - O5	169.0(4)	O1 - Yb1 - O9	96.4(4)
O1 - Yb1 - O3b	82.6(4)	O1 - Yb1 - O28c	87.5(4)
O1W - Yb1 - O2W	72.0(5)	O1W - Yb1 - O5	87.7(4)
O1W - Yb1 - O9	142.8(4)	O1W - Yb1 - O3b	144.1(4)
O1W - Yb1 - O28c	71.5(4)	O2W - Yb1 - O5	84.1(5)
O2W - Yb1 - O9	145.1(5)	O2W - Yb1 - O3b	76.4(4)
O2W - Yb1 - O28c	143.2(4)	O5 - Yb1 - O9	93.0(4)
O3b - Yb1 - O5	105.9(5)	O5 - Yb1 - O28c	90.2(5)
O3b - Yb1 - O9	71.0(4)	O9 - Yb1 - O28c	71.3(4)
O3b - Yb1 - O28c	139.5(4)	O3W - Yb2 - O4W	72.6(4)
O3W - Yb2 - O11	95.4(4)	O3W - Yb2 - O13	73.8(4)
O3W - Yb2 - O28	74.6(4)	O3W - Yb2 - O7a	144.0(4)
O3W - Yb2 - O15b	138.5(4)	O4W - Yb2 - O11	80.0(5)
O4W - Yb2 - O13	93.4(4)	O4W - Yb2 - O28	139.2(4)
O4W - Yb2 - O7a	143.1(4)	O4W - Yb2 - O15b	74.3(4)
O11 - Yb2 - O13	168.7(4)	O11 - Yb2 - O28	79.6(5)
O7a - Yb2 - O11	96.3(4)	O11 - Yb2 - O15b	102.8(5)
O13 - Yb2 - O28	100.2(4)	O7a - Yb2 - O13	94.5(4)
O13 - Yb2 - O15b	83.9(4)	O7a - Yb2 - O28	74.2(4)
O15b - Yb2 - O28	145.0(4)	O7a - Yb2 - O15b	70.8(4)

Symmetry transformations used to generate equivalent atoms: a: x,-2+y, z; b: x,-1+y, z; c x,1+y,z.

Table S7 Hydrogen bonds in **Ir₄Yb₂**

D-H···A	<i>d</i> (D-H) (Å)	<i>d</i> (H···A) (Å)	<i>d</i> (D···A) (Å)	∠ DHA (°)
O1W-H1WA···O3W ⁱ	0.8500	2.0600	2.897(17)	171.00
O1W-H1WB···O10 ⁱ	0.8500	1.9100	2.703(16)	154.00
O2W-H2WA···O4 ⁱⁱ	0.8500	1.8300	2.628(19)	157.00
O2W-H2WB···O24	0.8500	1.9800	2.69(2)	140.00
O3W-H3WB···O8 ⁱⁱ	0.8500	1.8800	2.679(16)	157.00
O3W-H3WC···O6W	0.8500	2.0000	2.81(3)	159.00
O4W-H4WA···O16 ⁱⁱ	0.8500	1.9000	2.600(17)	139.00
O4W-H4WB···O25 ⁱⁱ	0.8500	2.0800	2.68(3)	128.00
O5W-H5WB···O16 ⁱ	0.8500	2.0300	2.76(2)	142.00
O5W-H5WC···O25 ⁱ	0.8500	2.0300	2.87(2)	169.00
O24-H24A···O5W	0.8400	1.9600	2.69(2)	144.00
O25-H25B···O8W	0.8500	1.8700	2.57(5)	138.00
O26-H26A···O20 ⁱ	0.8400	2.1100	2.84(4)	145.00
O28-H28A···O11	0.8500	2.3800	2.848(19)	115.00

Symmetry transformations used to generate equivalent atoms: i: x, 1+y, z; ii: x, -1+y, z.

Table S8. Cell parameters of **Ir₂Gd** and **Ir₄Ln₂** (Ln = Gd, Dy, Er) were obtained by LeBail fitting the powder X-ray diffraction patterns (a) or single crystal X-ray diffraction analyses at 150 K (b).

	Ir₂Gd^a	Ir₄Gd₂^a	Ir₄Dy₂^a	Ir₄Dy₂^b	Ir₄Er₂^a	Ir₄Er₂^b
crystal system	Triclinic	Monoclinic	Monoclinic	Monoclinic	Monoclinic	Monoclinic
space group	<i>P</i> $\bar{1}$	<i>P</i> 2 ₁ /c				
<i>a</i> [Å]	8.5118	36.6123	36.6427	36.5349	36.5234	36.5048
<i>b</i> [Å]	18.4308	8.7589	8.6936	8.6464	8.6886	8.6197
<i>c</i> [Å]	23.9822	44.0515	43.9847	44.0538	44.0465	43.7404
α [°]	71.3693	90	90	90	90	90
β [°]	80.5212	112.3939	112.371	112.141	112.5198	112.256
γ [°]	77.9817	90	90	90	90	90
<i>V</i> [Å ³]	3467.4	13061.37	12957.23	12890.18	12911.90	12738.01
<i>Rwp</i> %	7.32	5.55	9.55	/	2.04	/

Table S9 The parameters obtained by Cole-Cole fitting for **Ir₂Dy** under zero dc field.

T / K	$\chi_s / \text{cm}^3 \text{K mol}$	$\chi_T / \text{cm}^3 \text{K mol}$	τ / s	α
1.8	1.494	5.329	3.39×10^{-5}	0.362
2	1.349	4.854	3.20×10^{-5}	0.369
2.2	1.261	4.452	3.09×10^{-5}	0.369
2.4	1.199	4.109	2.99×10^{-5}	0.367
2.6	1.151	3.817	2.89×10^{-5}	0.365
2.8	1.107	3.565	2.78×10^{-5}	0.364
3	1.071	3.345	2.68×10^{-5}	0.363
3.3	1.038	3.058	2.56×10^{-5}	0.356
3.6	1.010	2.819	2.44×10^{-5}	0.351
3.9	0.986	2.615	2.34×10^{-5}	0.346

Table S10 The parameters obtained by Cole-Cole fitting for **Ir₂Dy** under 2.0 kOe dc field.

T / K	χ_s	$\Delta\chi_1 / \text{cm}^3 \cdot \text{mol}^{-1}$	τ_1 / s	α_1	$\Delta\chi_2 / \text{cm}^3 \cdot \text{mol}^{-1}$	τ_2 / s	α_2
5.4	0.523	0.091	1.78×10^{-5}	0	1.401	0.00321	0.602
6	0.557	0.102	1.86×10^{-5}	0	1.098	0.00158	0.554
6.5	0.507	0.069	1.41×10^{-5}	0	1.169	0.00108	0.620
7	0.582	0.109	1.83×10^{-5}	0	0.822	6.54×10^{-4}	0.533
7.5	0.595	0.116	1.82×10^{-5}	0	0.722	4.96×10^{-4}	0.533

Table S11 The parameters obtained by Cole-Cole fitting for **Ir₄Dy₂** under zero dc field.

T / K	$\chi_s / \text{cm}^3 \text{K mol}$	$\chi_T / \text{cm}^3 \text{K mol}$	τ / s	α
1.8	6.36	14.28	7.34×10^{-5}	0.446
2	5.89	12.86	7.30×10^{-5}	0.449
2.2	5.48	11.71	7.23×10^{-5}	0.454
2.4	5.18	10.73	7.22×10^{-5}	0.453
2.6	4.94	9.90	7.22×10^{-5}	0.451
2.8	4.70	9.21	7.17×10^{-5}	0.450
3	4.53	8.58	7.13×10^{-5}	0.449
3.3	4.28	7.80	6.95×10^{-5}	0.445
3.6	4.09	7.14	6.80×10^{-5}	0.435
4	3.86	6.42	6.47×10^{-5}	0.421
4.5	3.50	5.74	5.42×10^{-5}	0.433
5	3.36	5.14	5.06×10^{-5}	0.379
5.5	3.08	4.69	3.92×10^{-5}	0.391
6	2.89	4.31	3.23×10^{-5}	0.383
7	2.48	3.72	1.85×10^{-5}	0.406
8	2.44	3.21	1.91×10^{-5}	0.255
9	2.21	2.88	1.33×10^{-5}	0.266

Table S12 The parameters obtained by Cole-Cole fitting for **Ir₄Dy₂** under 2.0 kOe dc field.

T / K	$\chi_s/\text{cm}^3 \text{ K mol}$	$\chi_T/\text{cm}^3 \text{ K mol}$	τ/s	α
1.8	0.935	9.510	6.18×10^{-4}	0.522
2	1.046	9.200	6.12×10^{-4}	0.528
2.2	1.164	8.853	5.96×10^{-4}	0.529
2.4	1.260	8.495	5.71×10^{-4}	0.532
2.6	1.367	8.106	5.36×10^{-4}	0.529
2.8	1.414	7.796	5.06×10^{-4}	0.535
3	1.499	7.448	4.71×10^{-4}	0.531
3.3	1.586	6.942	4.07×10^{-4}	0.525
3.6	1.647	6.480	3.44×10^{-4}	0.517
4	1.688	6.057	2.87×10^{-4}	0.507
4.2	1.672	5.753	2.45×10^{-4}	0.509
4.5	1.720	5.356	1.98×10^{-4}	0.486
5	1.711	4.872	1.44×10^{-4}	0.467
5.5	1.581	4.567	1.05×10^{-4}	0.487
6	1.579	4.203	7.99×10^{-5}	0.466
6.5	1.593	3.895	6.47×10^{-5}	0.442
7	1.640	3.587	5.39×10^{-5}	0.396
8	1.526	3.203	3.57×10^{-5}	0.401
9	1.561	2.831	2.91×10^{-5}	0.333
10	1.519	2.565	2.32×10^{-5}	0.307
11	1.511	2.339	2.02×10^{-5}	0.253
12	1.448	2.145	1.64×10^{-5}	0.229
13	1.408	1.985	1.35×10^{-5}	0.196

Table S13 The parameters obtained by Cole-Cole fitting for **Ir₂Er** under 1.0 kOe dc field.

T / K	$\chi_s / \text{cm}^3 \text{ K mol}$	$\chi_T / \text{cm}^3 \text{ K mol}$	τ / s	α
1.8	1.139	3.211	5.25×10^{-5}	0.095
2	1.061	2.939	2.42×10^{-5}	0.105
2.2	1.034	2.718	1.19×10^{-5}	0.122
2.4	1.131	2.533	7.03×10^{-5}	0.140
2.6	1.356	2.369	5.59×10^{-6}	0.135

Table S14 The parameters obtained by Cole-Cole fitting for **Ir₄Er₂** under 1.5 kOe dc field.

T / K	$\chi_s / \text{cm}^3 \text{ K mol}$	$\chi_T / \text{cm}^3 \text{ K mol}$	τ / s	α
1.8	1.508	6.348	4.47×10^{-5}	0.107
2	1.431	5.870	2.53×10^{-5}	0.109
2.2	1.456	5.459	1.44×10^{-5}	0.114
2.4	1.603	5.106	8.82×10^{-6}	0.123
2.6	1.912	4.798	6.14×10^{-6}	0.129

Table S15 The parameters obtained by Cole-Cole fitting for **Ir₂Yb** under 2.0 kOe dc field.

T / K	$\chi_s / \text{cm}^3 \text{ K mol}$	$\chi_T / \text{cm}^3 \text{ K mol}$	τ / s	α
1.8	0.2105	0.703	9.29×10^{-4}	0.170
2	0.200	0.637	7.61×10^{-4}	0.146
2.2	0.186	0.582	6.33×10^{-4}	0.142
2.4	0.173	0.537	5.28×10^{-4}	0.142
2.6	0.164	0.496	4.37×10^{-4}	0.125
2.8	0.158	0.461	3.64×10^{-4}	0.104
3	0.150	0.436	3.08×10^{-4}	0.099
3.3	0.131	0.409	2.32×10^{-4}	0.133
3.6	0.118	0.374	1.63×10^{-4}	0.130
4	0.127	0.336	1.25×10^{-4}	0.038
4.2	0.084	0.324	7.23×10^{-5}	0.167
4.5	0.078	0.304	5.28×10^{-5}	0.163
5	0.074	0.276	3.27×10^{-5}	0.143
5.5	0.085	0.242	2.26×10^{-5}	0.032
6	0.087	0.222	1.62×10^{-5}	8.50×10^{-8}
6.5	0.081	0.206	1.11×10^{-5}	7.88×10^{-8}

Table S16 The parameters obtained by Cole-Cole fitting for **Ir₄Yb₂** under 1.5 kOe dc field.

T / K	χ_s	$\Delta\chi_1 / \text{cm}^3 \cdot \text{mol}^{-1}$	τ_1 / s	α_1	$\Delta\chi_2 / \text{cm}^3 \cdot \text{mol}^{-1}$	τ_2 / s	α_2
1.8	0.222	0.721	6.47×10^{-5}	0.25	0.327	9.23×10^{-4}	5.3×10^{-6}
2	0.205	0.685	5.80×10^{-5}	0.25	0.288	7.96×10^{-4}	8.3×10^{-4}
2.2	0.200	0.628	5.16×10^{-5}	0.23	0.269	6.79×10^{-4}	1.2×10^{-5}
2.4	0.194	0.579	4.62×10^{-5}	0.21	0.248	5.78×10^{-4}	2.4×10^{-5}
2.6	0.163	0.606	4.41×10^{-5}	0.26	0.196	5.42×10^{-4}	4.1×10^{-5}
2.8	0.171	0.529	3.82×10^{-5}	0.21	0.202	4.46×10^{-4}	6.3×10^{-5}
3	0.174	0.475	3.34×10^{-5}	0.17	0.202	3.68×10^{-4}	8.7×10^{-5}
3.3	0.145	0.489	2.92×10^{-5}	0.22	0.156	3.09×10^{-4}	2.6×10^{-5}
3.6	0.123	0.490	2.48×10^{-5}	0.25	0.125	2.47×10^{-4}	4.0×10^{-5}
3.9	0.148	0.387	1.97×10^{-5}	0.15	0.144	1.76×10^{-4}	8.6×10^{-5}
4.2	0.141	0.372	1.65×10^{-5}	0.16	0.125	1.39×10^{-4}	1.2×10^{-4}
4.5	0.089	0.454	1.34×10^{-5}	0.29	0.068	9.52×10^{-5}	1.3×10^{-11}
5	0.130	0.318	9.36×10^{-6}	0.14	0.096	6.45×10^{-5}	2.2×10^{-11}
5.5	0.056	0.380	4.86×10^{-6}	0.25	0.067	3.83×10^{-5}	2.6×10^{-29}
6	6.28×10^{-8}	0.385	1.91×10^{-6}	0.32	0.081	2.09×10^{-5}	1.9×10^{-29}
6.5	5.76×10^{-8}	0.327	1.94×10^{-6}	1.34×10^{-14}	0.093	1.79×10^{-5}	2.7×10^{-29}
7	7.64×10^{-8}	0.321	1.56×10^{-6}	1.47×10^{-14}	0.073	1.49×10^{-5}	3.5×10^{-29}

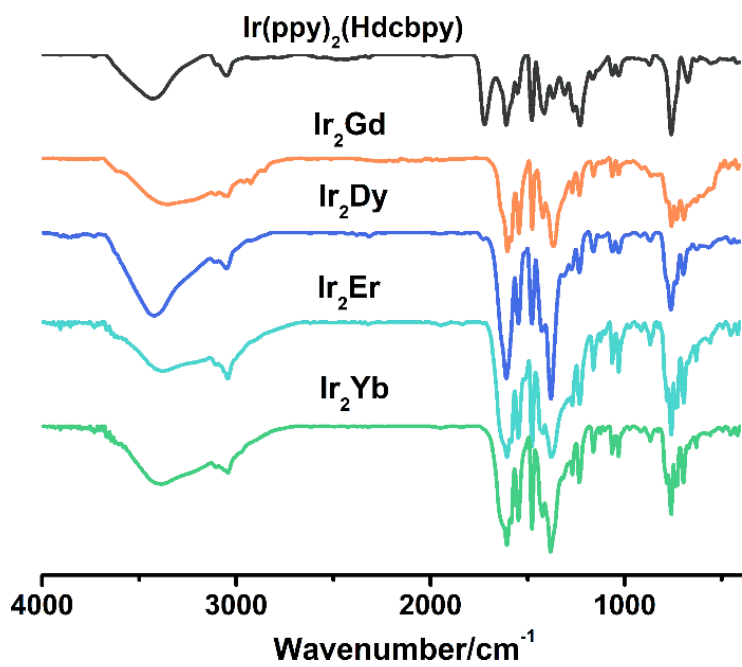


Figure S1. FT-IR spectra of compounds Ir_2Ln and the free ligand.

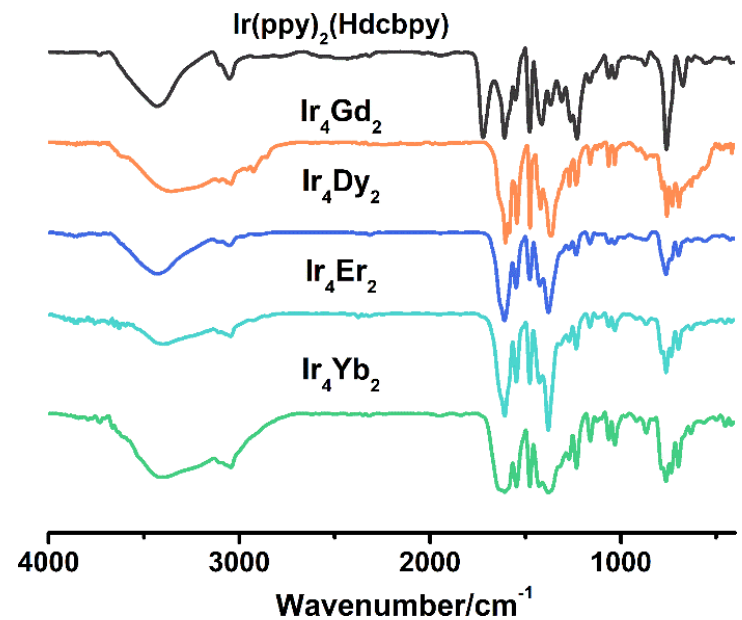


Figure S2. FT-IR spectra of compounds Ir_4Ln_2 and the free ligand.

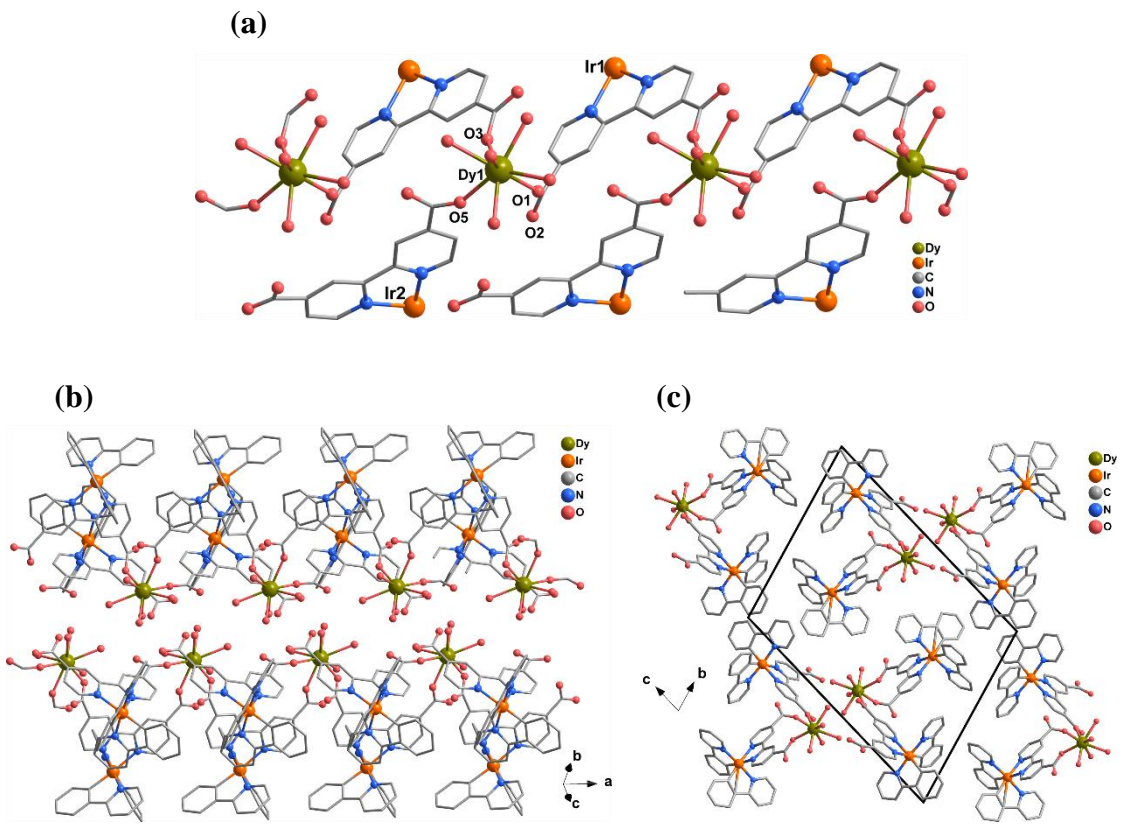


Figure S3. (a) One dimensional chain structure in compound **Ir₂Dy**. (b) The supramolecular double-chain of **Ir₂Dy**. (c) The 3D packing supramolecular framework of **Ir₂Dy** along the *a*-axis.

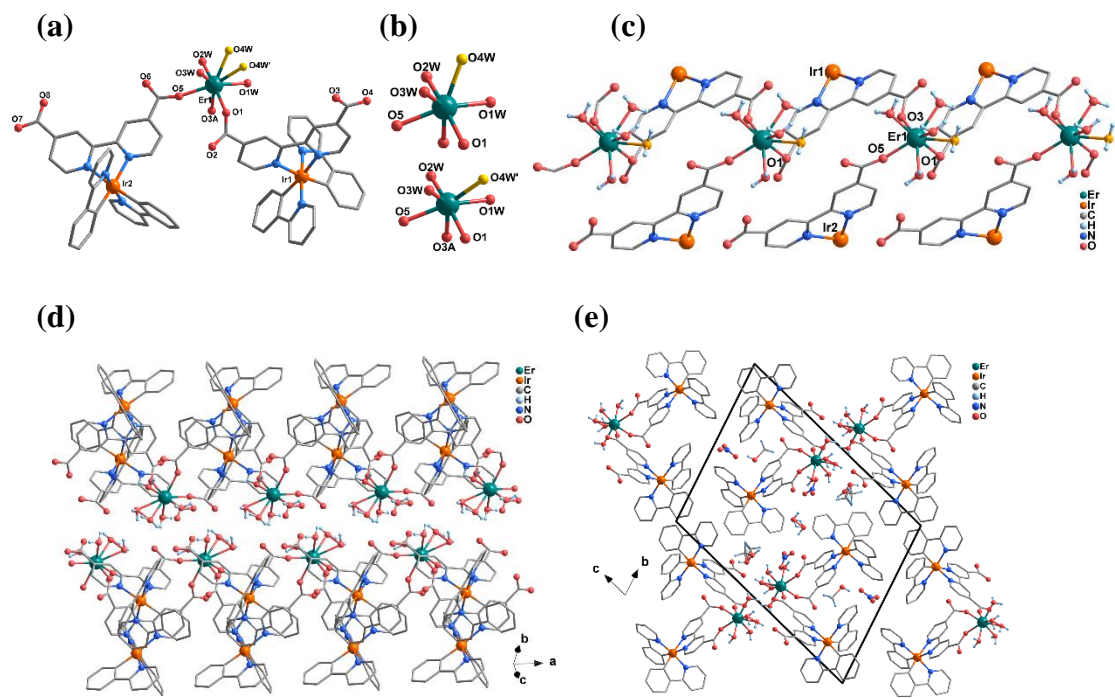


Figure S4. (a) Molecular structure of **Ir₂Er** and (b) Coordination environments of the Er(III) ions. (c) One dimensional chain structure in compound **Ir₂Er**. (d) The supramolecular double-chain of **Ir₂Er**. (e) The 3D packing supramolecular framework of **Ir₂Er** along the *a*-axis.

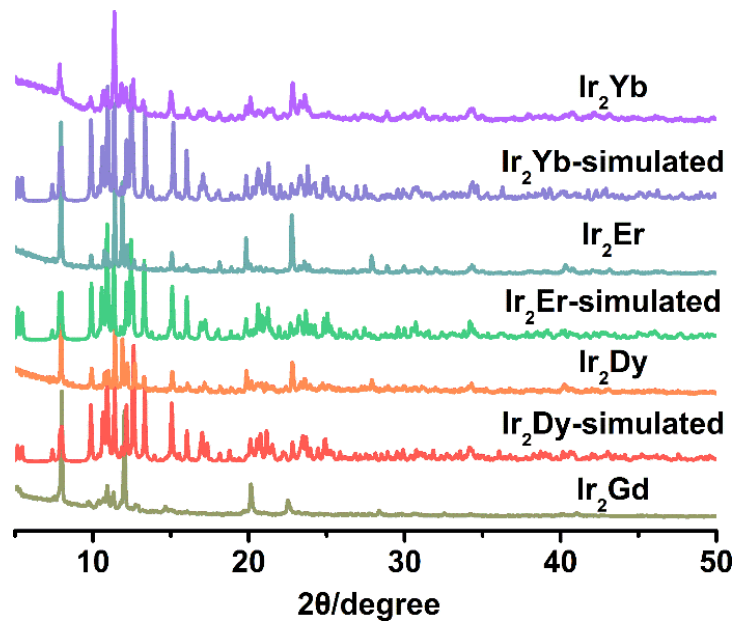


Figure S5. Simulated and experimental powder X-ray diffraction patterns of compounds Ir_2Ln .

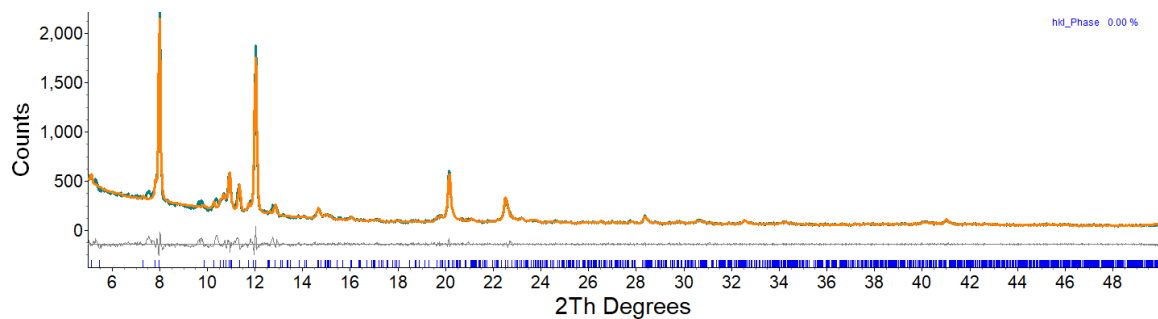


Figure S6. Pawley fit of a powder sample of compound Ir_2Gd performed using *Topas 5.0* program. Green is the measured intensities, orange is the calculated intensities, and gray is the difference plot between the measured and calculated intensities ($R_{wp} : 7.32\%$).

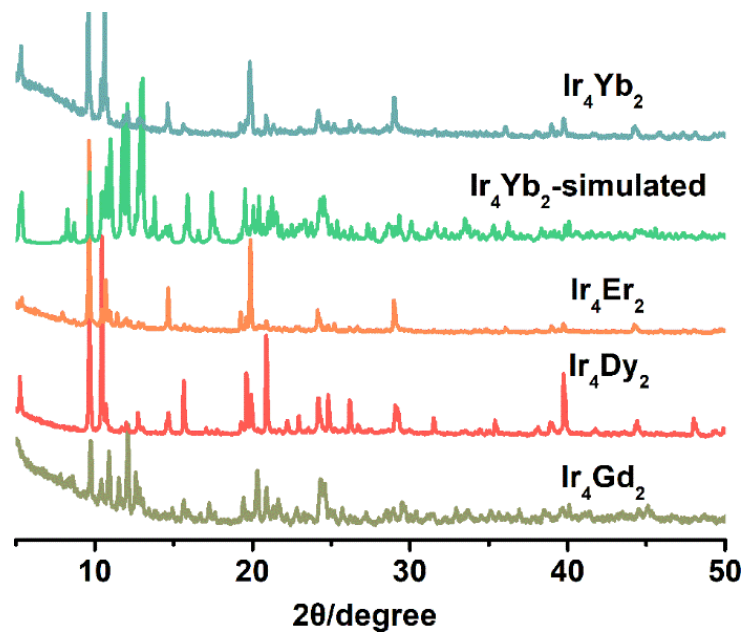


Figure S7. Simulated and experimental powder X-ray diffraction patterns of compounds Ir_4Ln_2 .

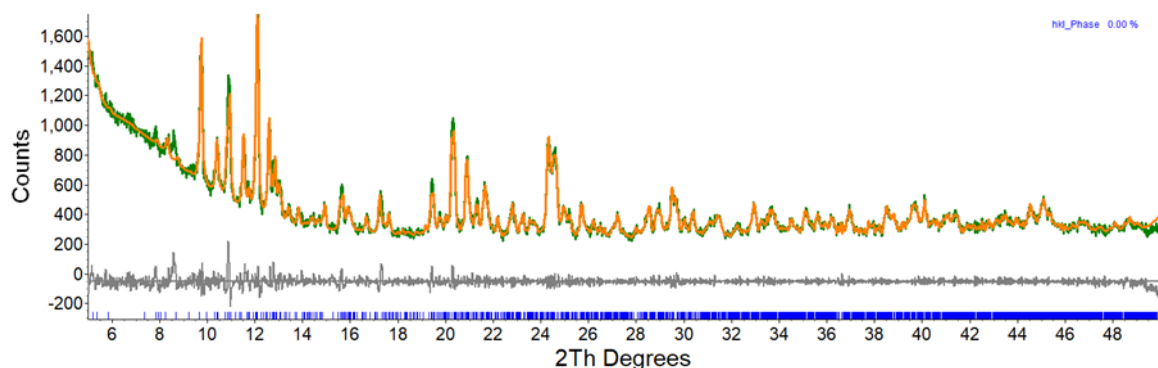


Figure S8. Pawley fit of a powder sample of compound Ir_4Gd_2 performed using *Topas 5.0* program. Green is the measured intensities, orange is the calculated intensities, and gray is the difference plot between the measured and calculated intensities (Rwp: 5.55%).

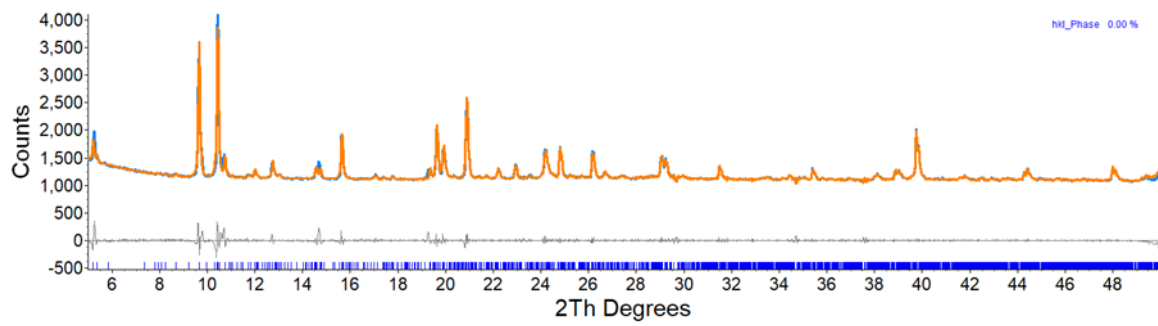


Figure S9. Pawley fit of a powder sample of compound **Ir₄Dy₂** performed using *Topas 5.0* program. Blue is the measured intensities, orange is the calculated intensities, and gray is the difference plot between the measured and calculated intensities (Rwp: 5.55%).

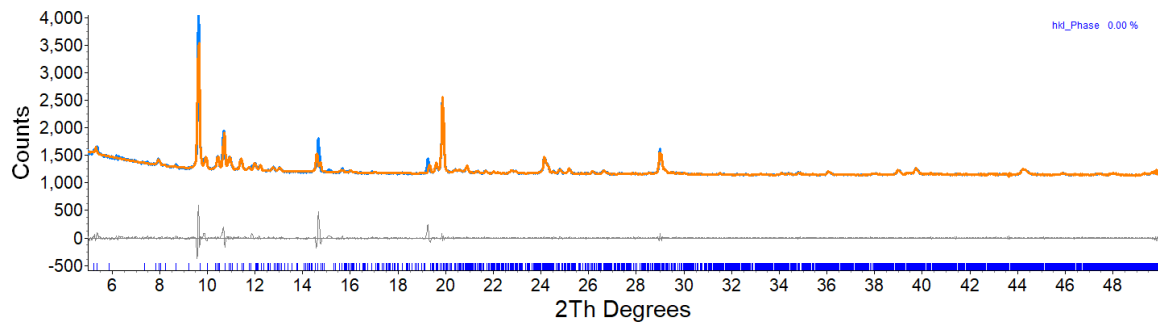


Figure S10. Pawley fit of a powder sample of compound **Ir₄Er₂** performed using *Topas 5.0* program. Blue is the measured intensities, orange is the calculated intensities, and gray is the difference plot between the measured and calculated intensities (Rwp: 2.04%).

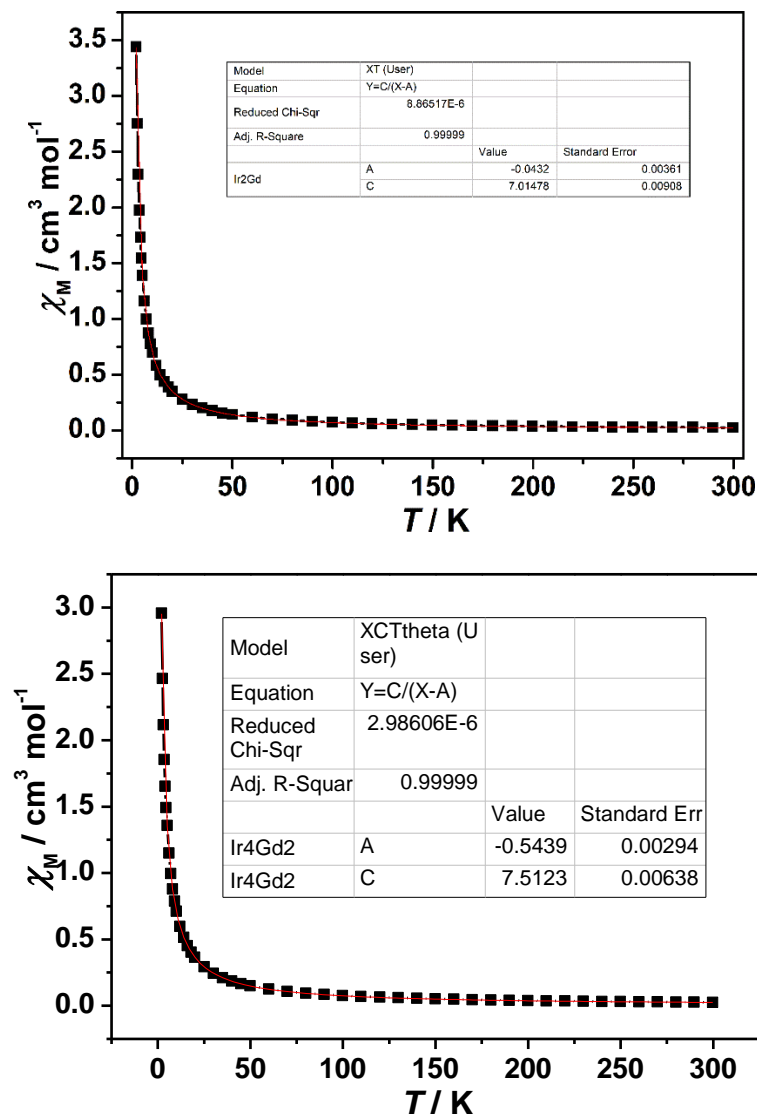


Figure S11. The χ_M vs. T curves for **Ir₂Gd** (top) and **Ir₄Gd₂** (bottom). The red solid lines represent the best fits of the data in the whole temperature range.

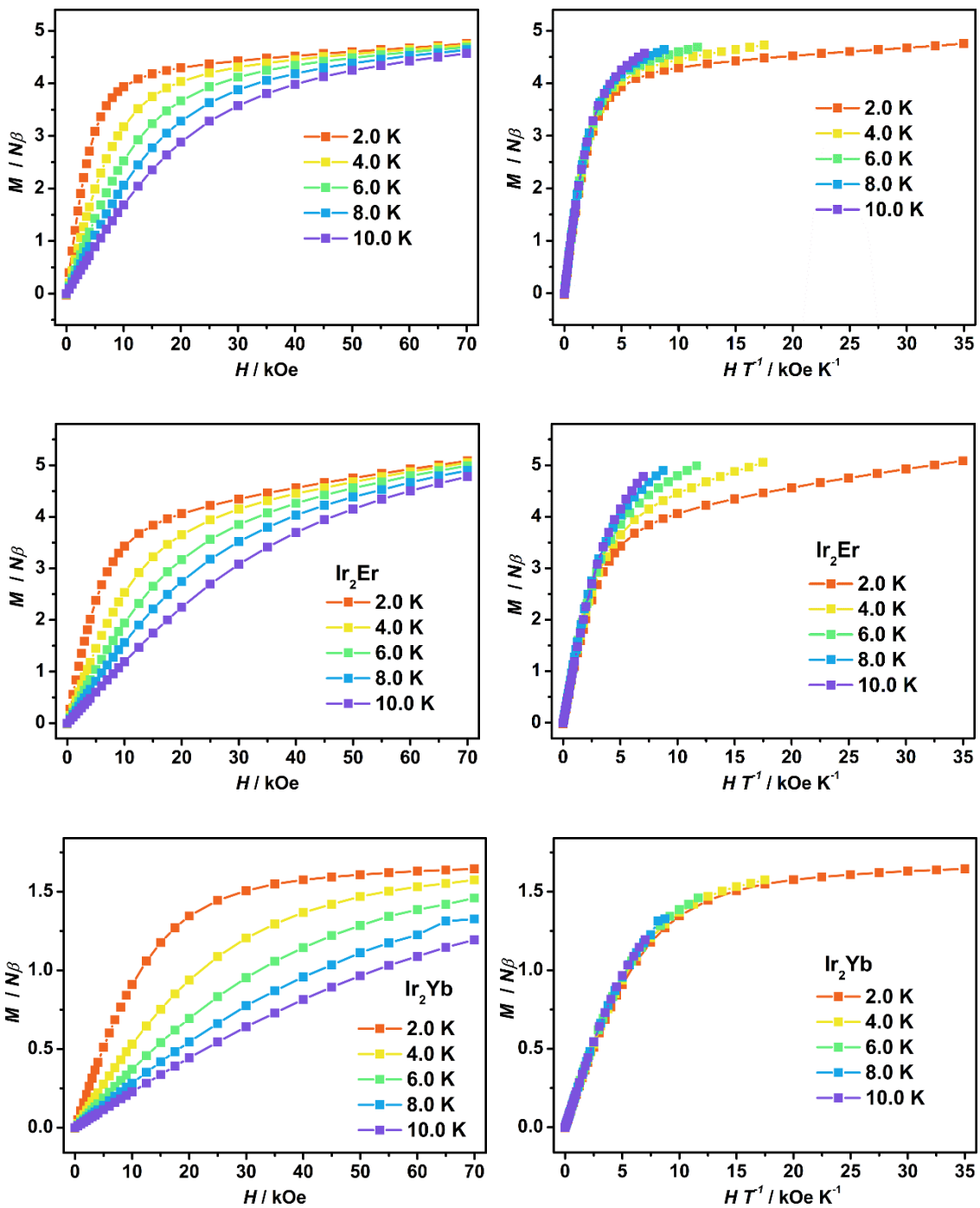


Figure S12. The plot of magnetization M vs. H and M vs. H/T at depicted temperatures for Ir_2Ln ($\text{Ln}=\text{Dy}, \text{Er}, \text{Yb}$).

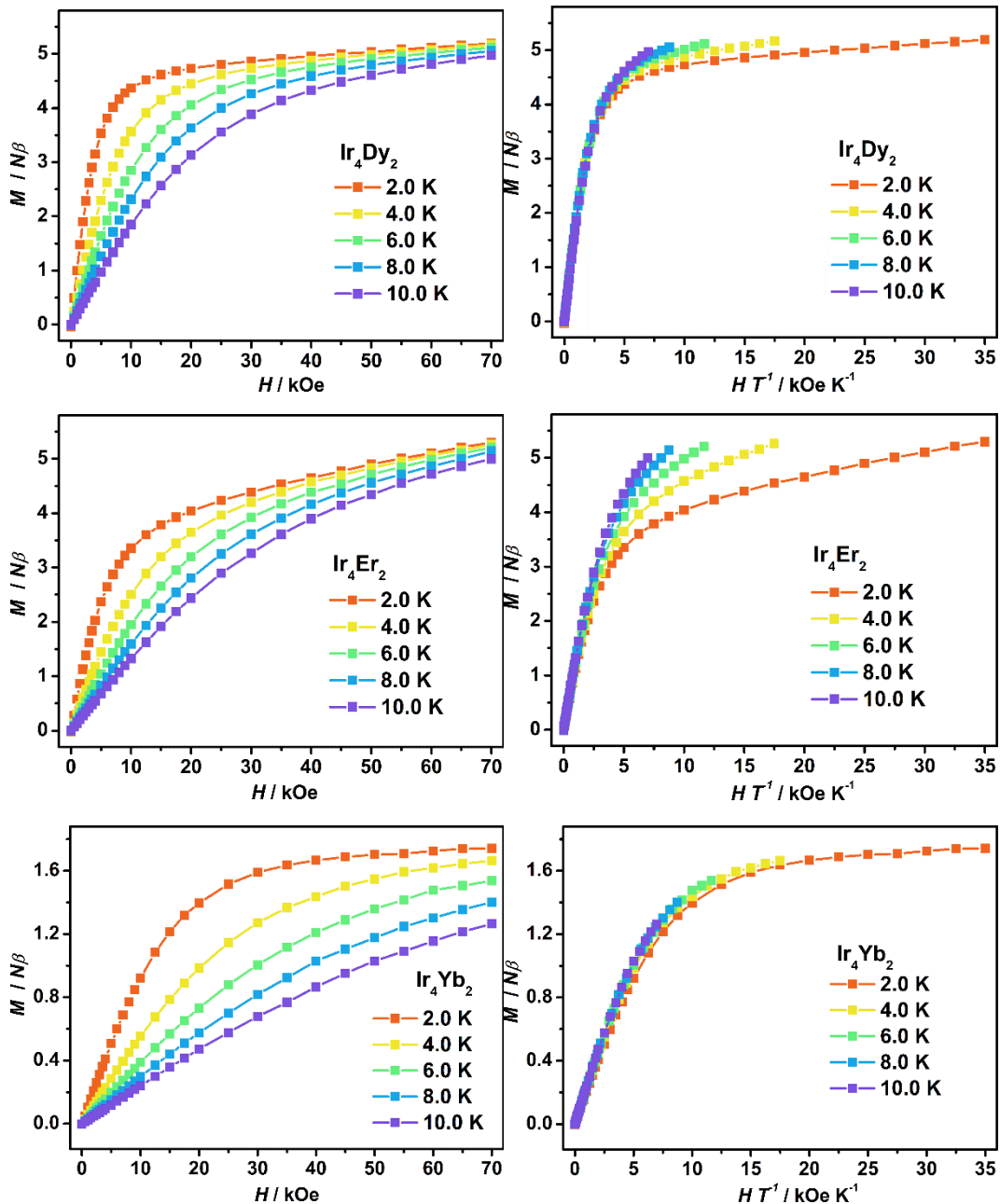


Figure S13. The plot of magnetization M vs. H and M vs. H/T at depicted temperatures for Ir_4Ln_2 ($\text{Ln} = \text{Dy}, \text{Er}, \text{Yb}$).

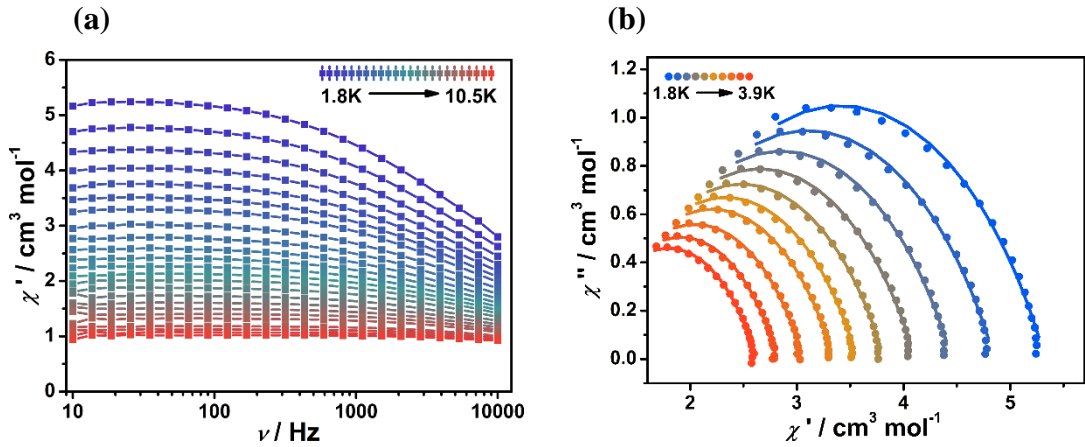


Figure S14. (a) The in-phase (χ') ac susceptibilities and (b) Cole-Cole plot of **Ir₂Dy** under zero dc field.

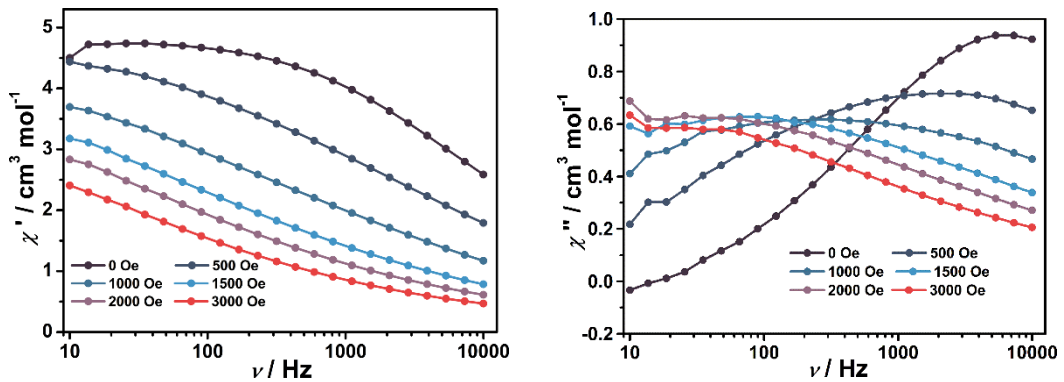


Figure S15. In-phase (χ') and out-of-phase (χ'') ac susceptibilities of **Ir₂Dy** collected at 1.8 K under dc fields ranging from 0 to 3.0 kOe.

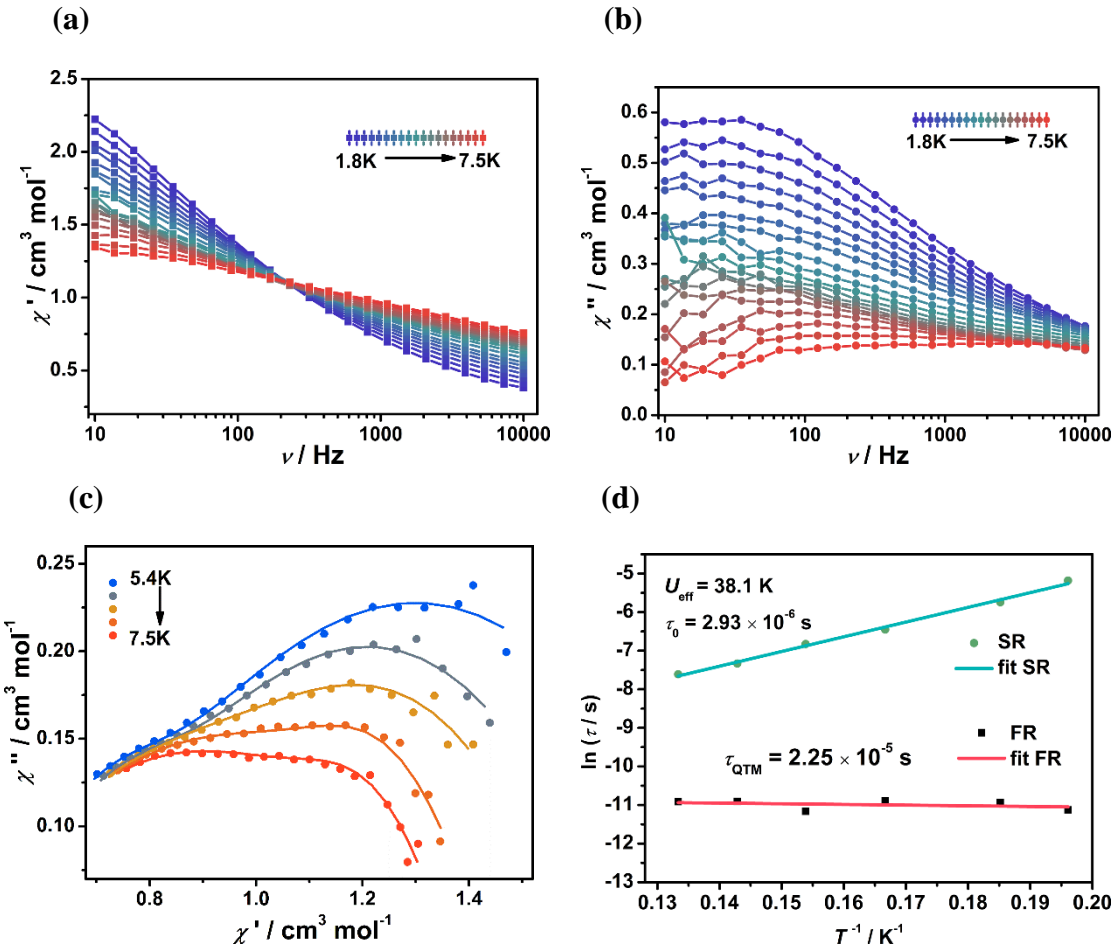


Figure S16. The ac susceptibilities for **Ir₂Dy** under 2.0 kOe dc field at different temperatures: (a) frequency dependence of in-phase (χ') and (b) out-of-phase (χ''), (c) Cole-Cole plot and (d) plots of $\ln(\tau)$ vs. $1/T$.

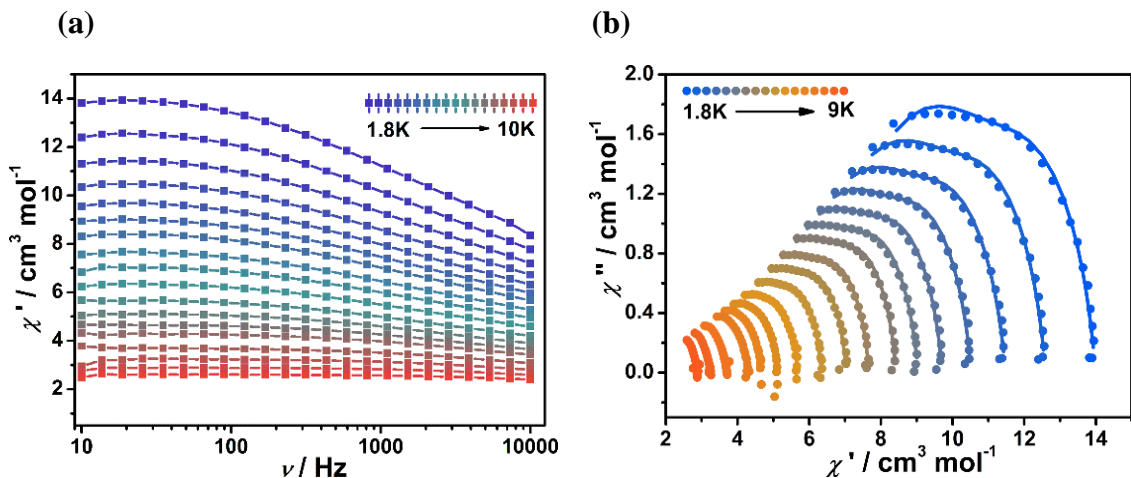


Figure S17. (a) The in-phase (χ') ac susceptibilities and (b) Cole-Cole plot of **Ir₄Dy₂** under zero dc field.

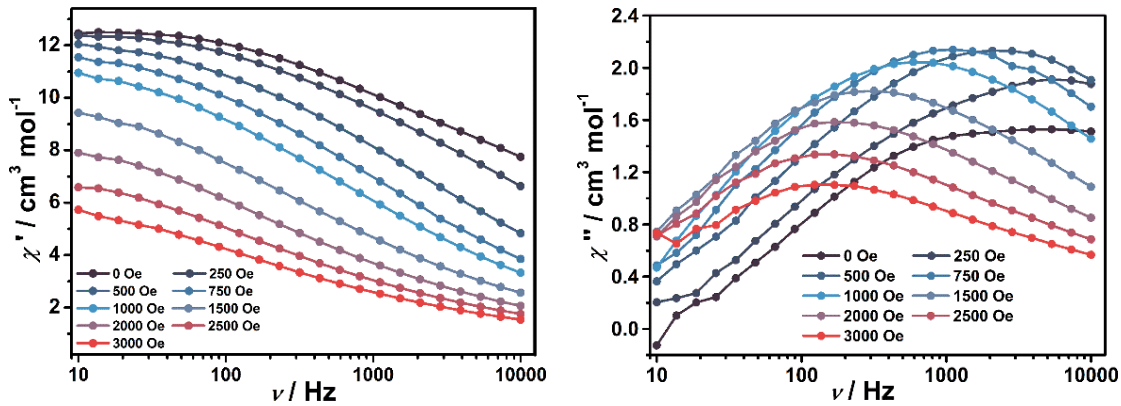


Figure S18. In-phase (χ') and out-of-phase (χ'') ac susceptibilities of Ir_4Dy_2 collected at 1.8 K under dc fields ranging from 0 to 3.0 kOe.

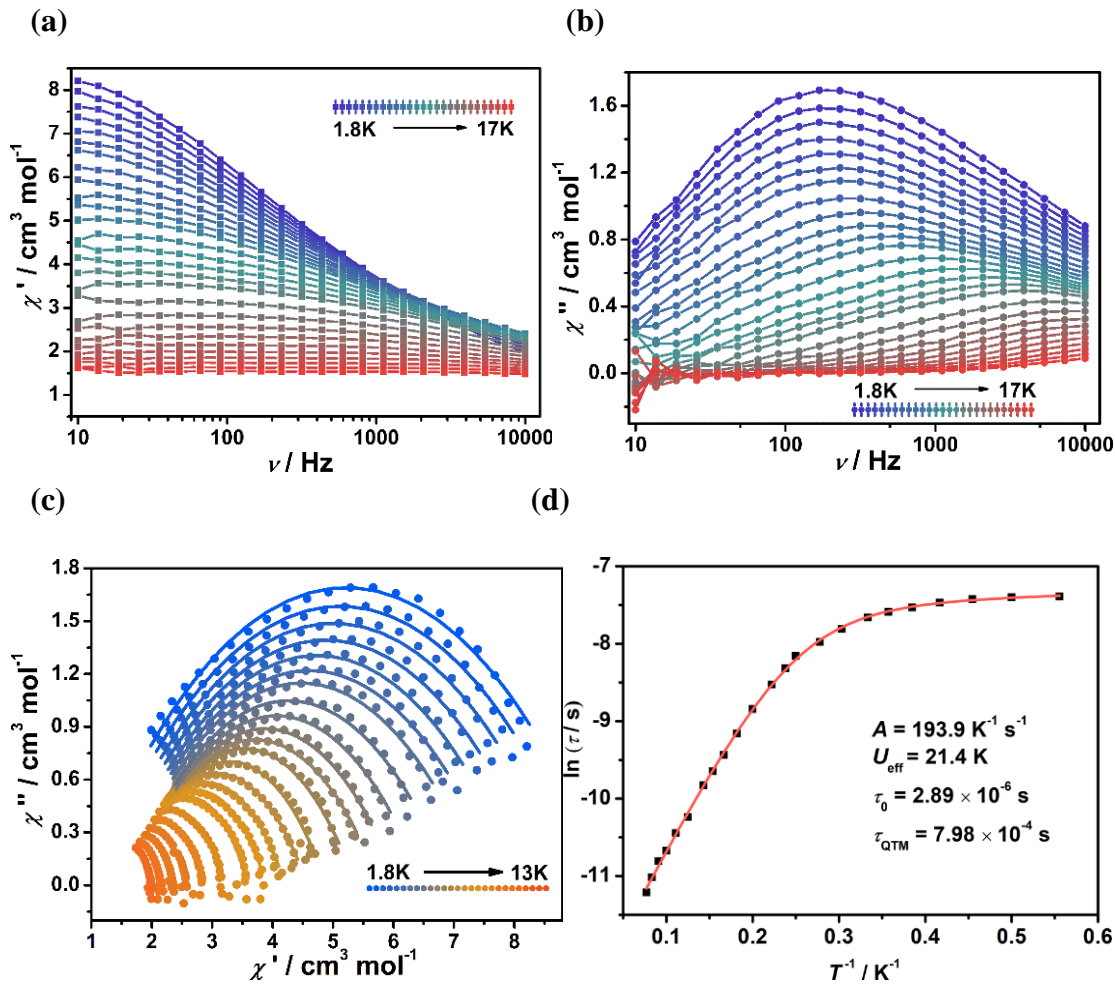


Figure S19. The ac susceptibility of Ir_4Dy_2 under a 2.0 kOe dc field at different temperatures: (a) frequency dependence of in-phase (χ') and (b) out-of-phase (χ''), (c) Cole-Cole plot and (d) plots of $\ln(\tau)$ vs. $1/T$.

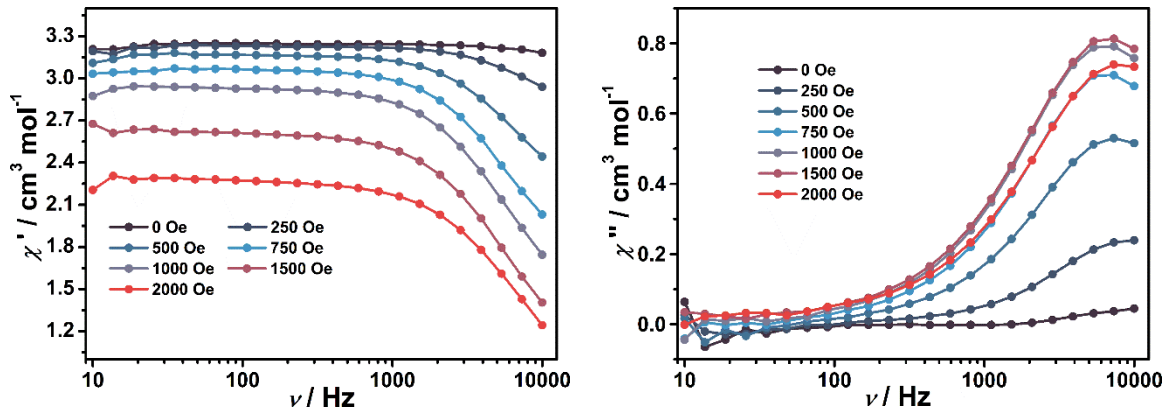


Figure S20. In-phase (χ') and out-of-phase (χ'') ac susceptibilities of Ir_2Er collected at 1.8 K under dc field ranging from 0 to 3.0 kOe.

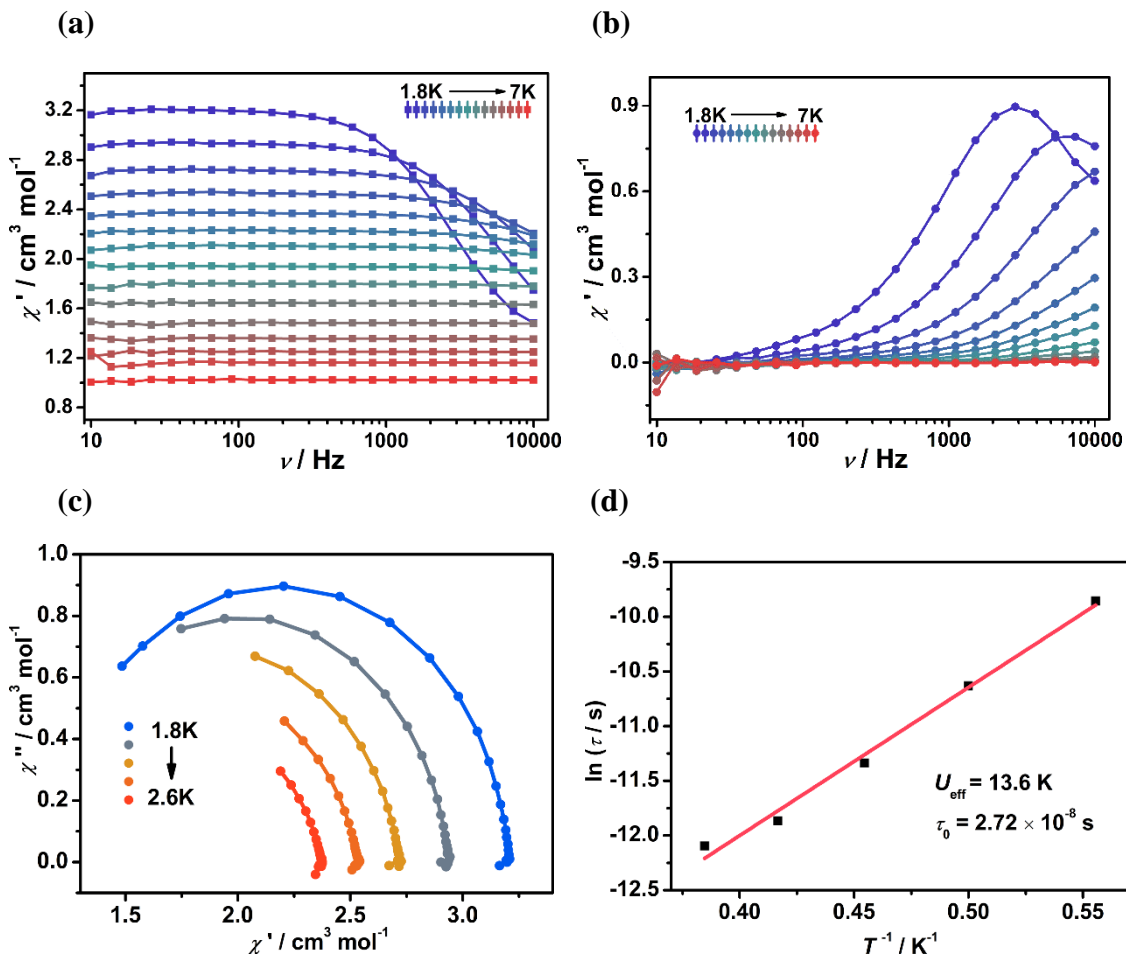


Figure S21. The ac susceptibilities of Ir_2Er under a 1.0 kOe dc field at different temperatures: (a) frequency dependence of in-phase (χ') and (b) out-of-phase (χ''), (c) Cole-Cole plot and (d) plots of $\ln(\tau)$ vs. $1/T$.

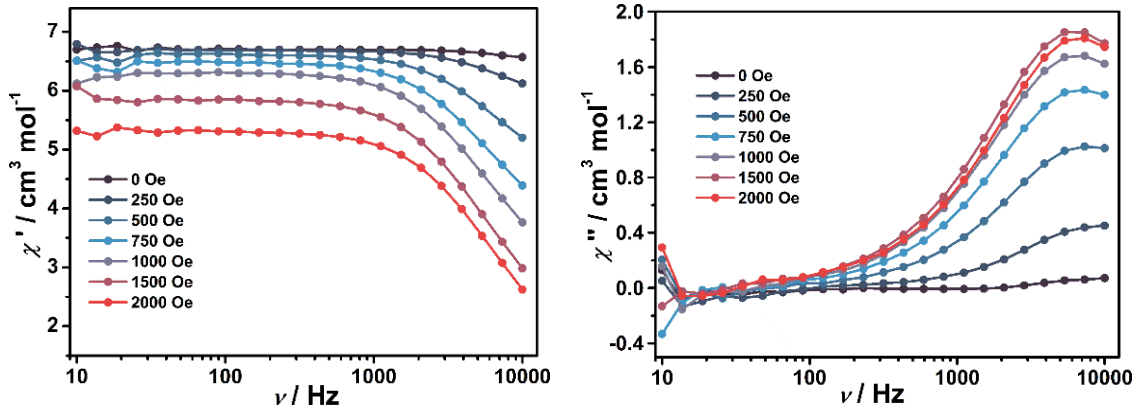


Figure S22. In-phase (χ') and out-of-phase (χ'') ac susceptibilities of Ir_4Er_2 collected at 1.8 K under dc field ranging from 0 to 3.0 kOe.

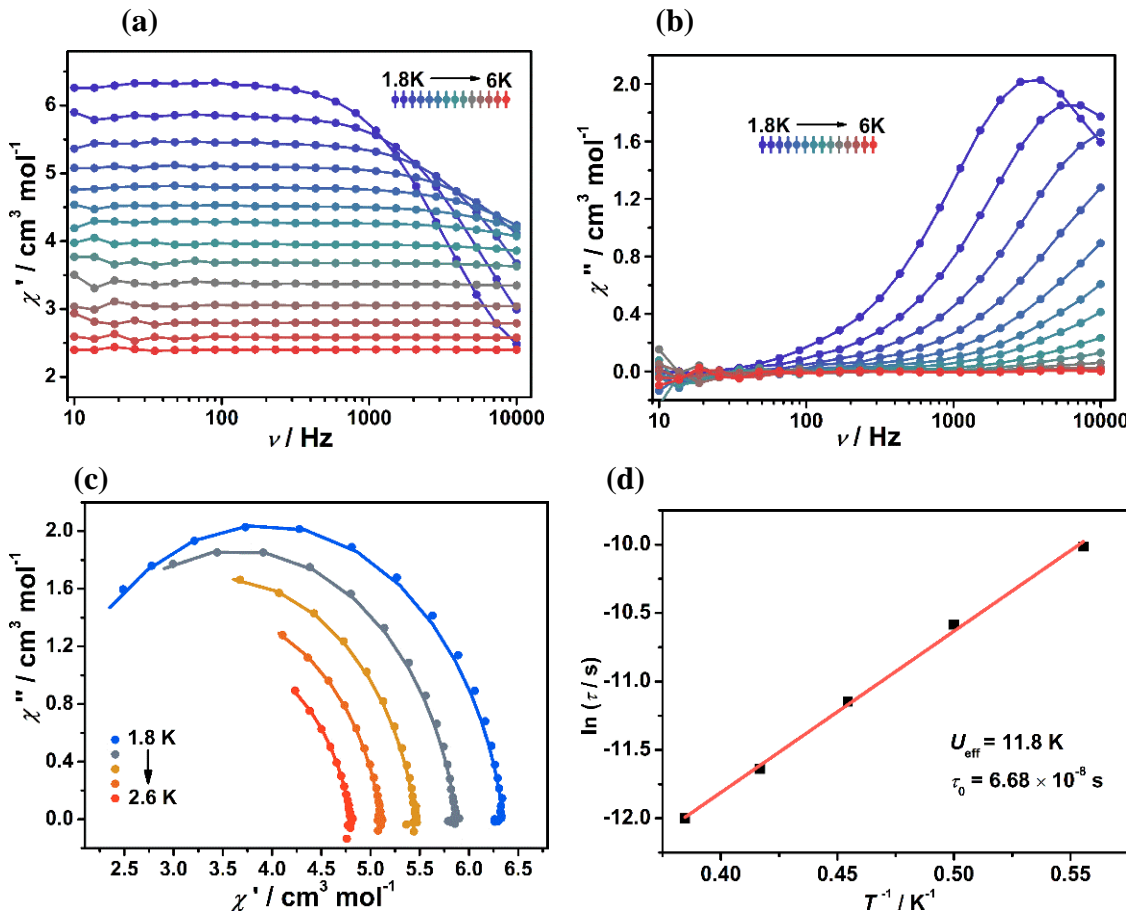


Figure S23. The ac susceptibilities of Ir_4Er_2 under a 1.5 kOe dc field at different temperatures: (a) frequency dependence of in-phase (χ') and (b) out-of-phase (χ''), (c) Cole-Cole plot and (d) plots of $\ln(\tau)$ vs. $1/T$.

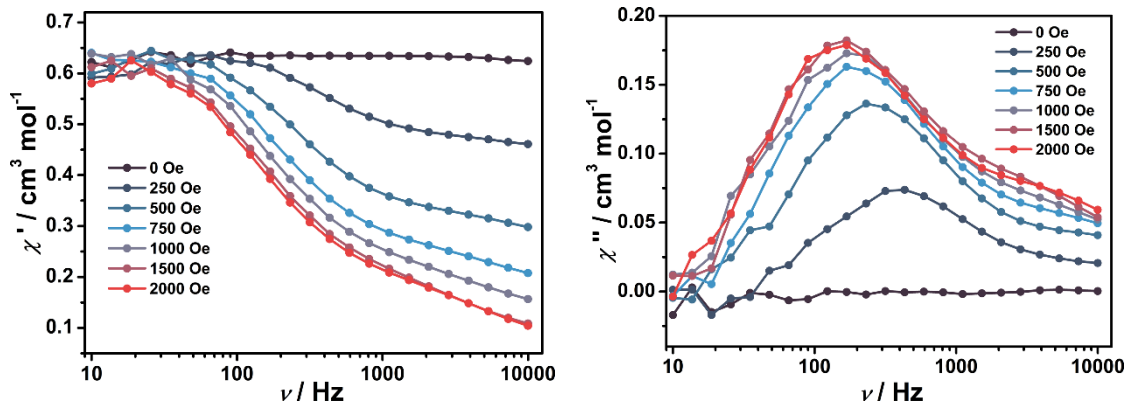


Figure S24. In-phase (χ') and out-of-phase ac susceptibility (χ'') of Ir_2Yb collected at 1.8 K under dc fields ranging from 0 to 3.0 kOe.

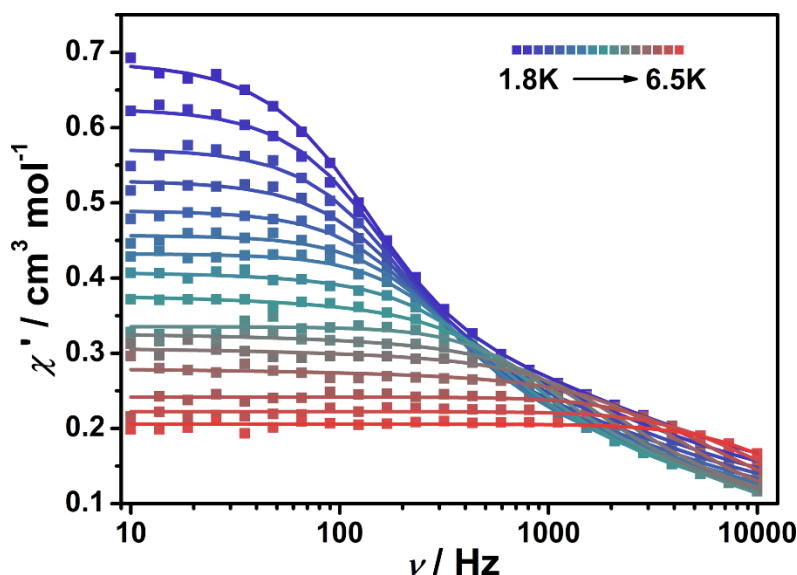


Figure S25. The in-phase (χ') ac susceptibilities of Ir_2Yb under a 1.0 kOe dc field at different temperatures.

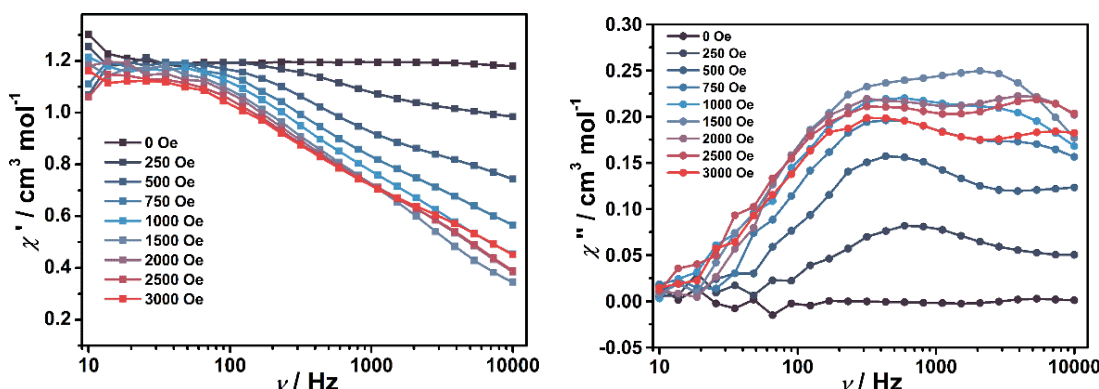


Figure S26. In-phase (χ') and out-of-phase (χ'') ac susceptibilities of Ir_4Yb_2 collected at 1.8 K under dc field ranging from 0 to 3.0 kOe.

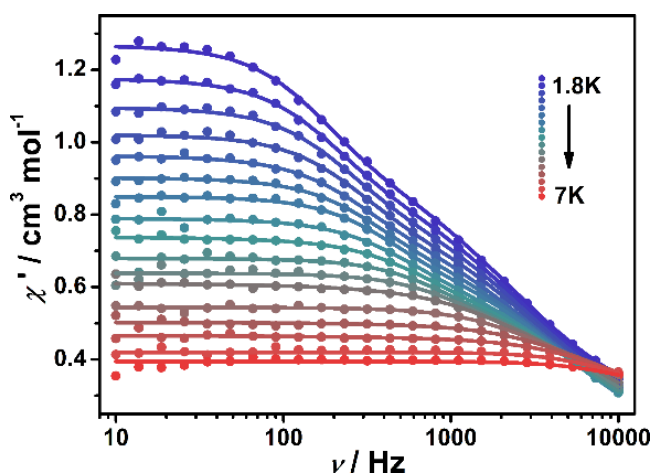


Figure S27. The in-phase (χ') ac susceptibilities of Ir_4Yb_2 under a 1.5 kOe dc field at different temperatures.

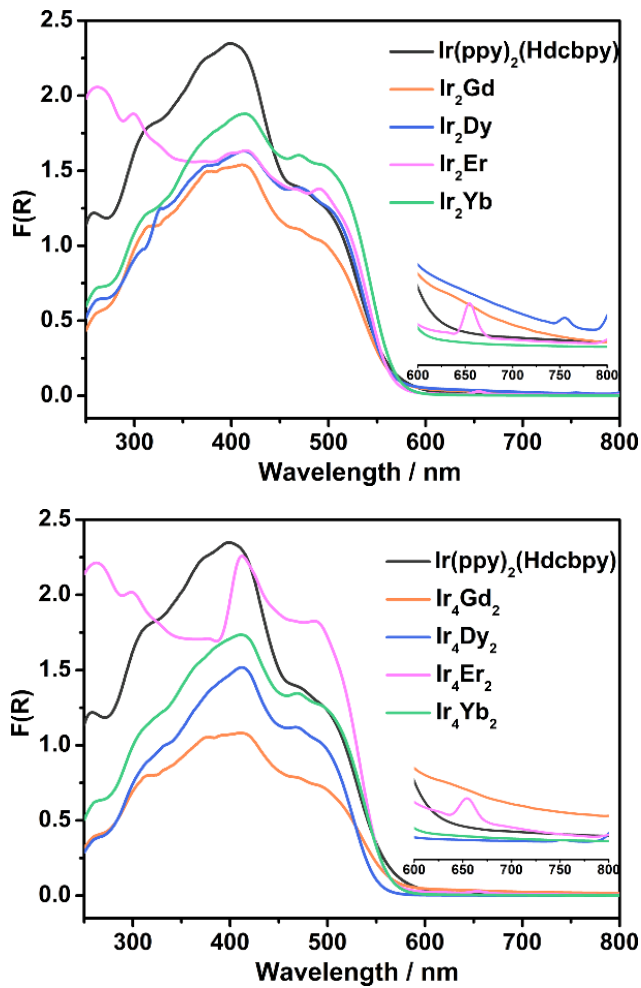


Figure S28. The absorption spectra of $\text{Ir}(\text{ppy})_2(\text{Hdcbpy})$ and of compounds Ir_2Ln and Ir_4Ln_2 ($\text{Ln} = \text{Gd}, \text{Dy}, \text{Er}, \text{Yb}$) in the solid-state.

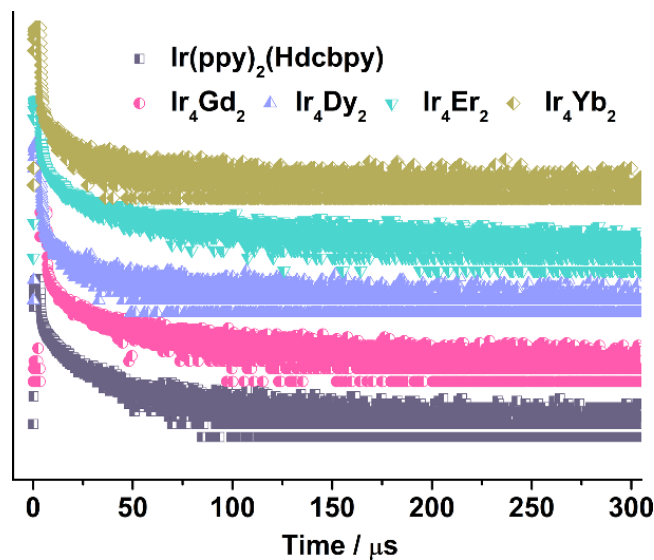
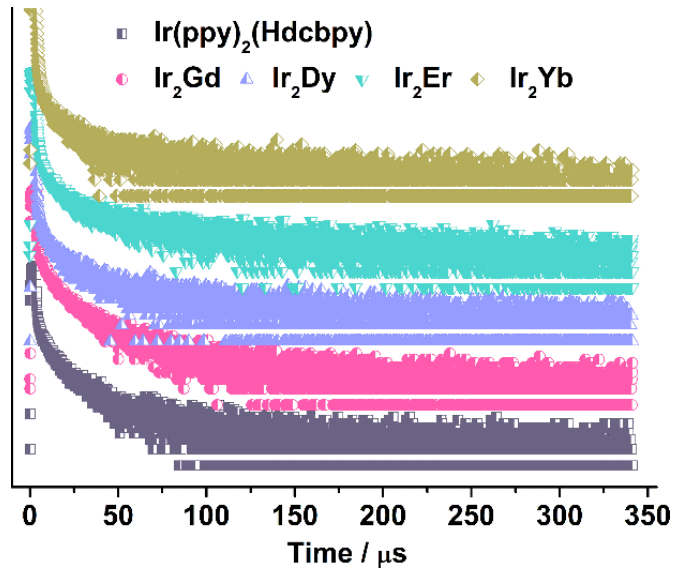


Figure S29. The luminescence decay for compounds $\text{Ir}(\text{ppy})_2(\text{Hdcbpy})$, **Ir₂Ln** and **Ir₄Ln₂** ($\text{Ln} = \text{Gd}, \text{Dy}, \text{Er}, \text{Yb}$) fitted by bi-exponential function $I = A + B_1\exp(-t/\tau_1) + B_2\exp(-t/\tau_2)$, affording lifetimes (τ) of 6.60 μs ($\chi^2 = 1.37$) for $\text{Ir}(\text{ppy})_2(\text{Hdcbpy})$, 8.69 μs ($\chi^2 = 1.27$) for **Ir₂Gd**, 4.79 μs ($\chi^2 = 1.43$) for **Ir₂Dy**, 6.37 μs ($\chi^2 = 1.47$) for **Ir₂Er**, 2.23 μs ($\chi^2 = 1.39$) for **Ir₂Yb**, 7.74 μs ($\chi^2 = 1.33$) for **Ir₄Gd₂**, 0.66 μs ($\chi^2 = 1.32$) for **Ir₄Dy₂**, 5.47 μs ($\chi^2 = 1.35$) for **Ir₄Er₂** and 1.24 μs ($\chi^2 = 1.20$) for **Ir₄Yb₂**.

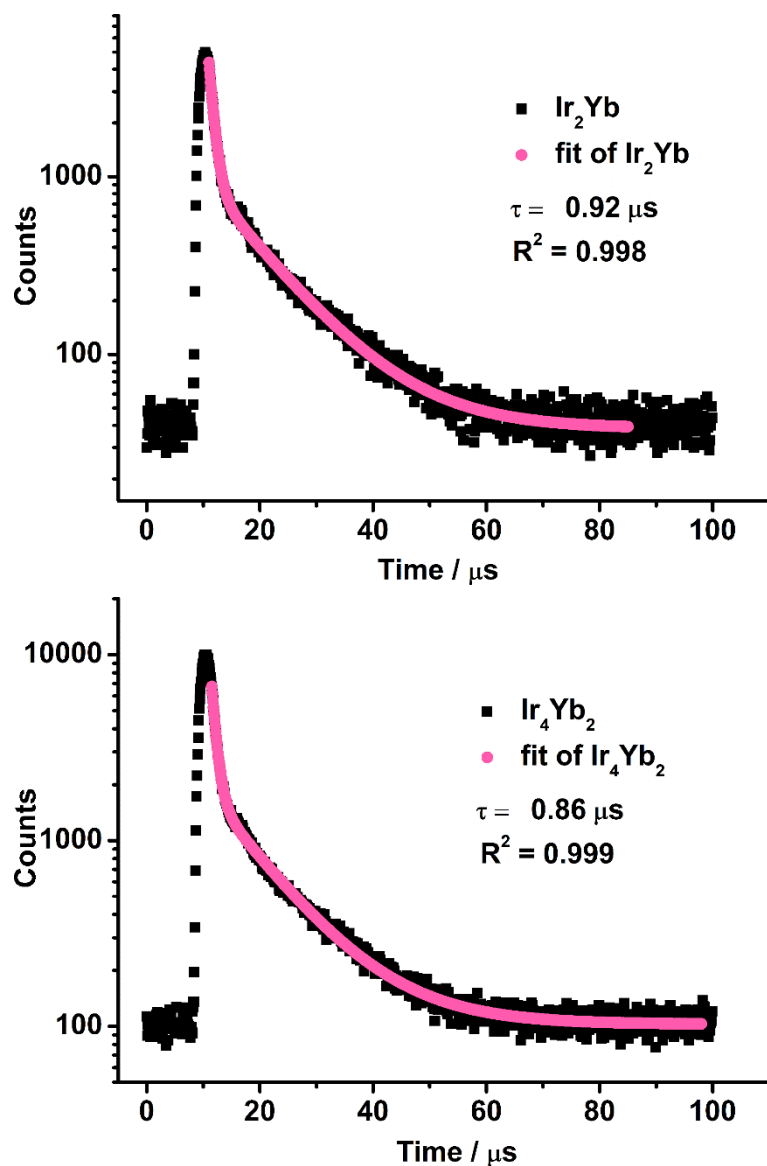


Figure S30. Luminescent decay profiles monitored at 975 nm for Ir_2Yb and Ir_4Yb_2 in the solid state at room temperature. The lifetime was fitted by bi-exponential function $I = A + B_1\exp(-t/\tau_1) + B_2\exp(-t/\tau_2)$.

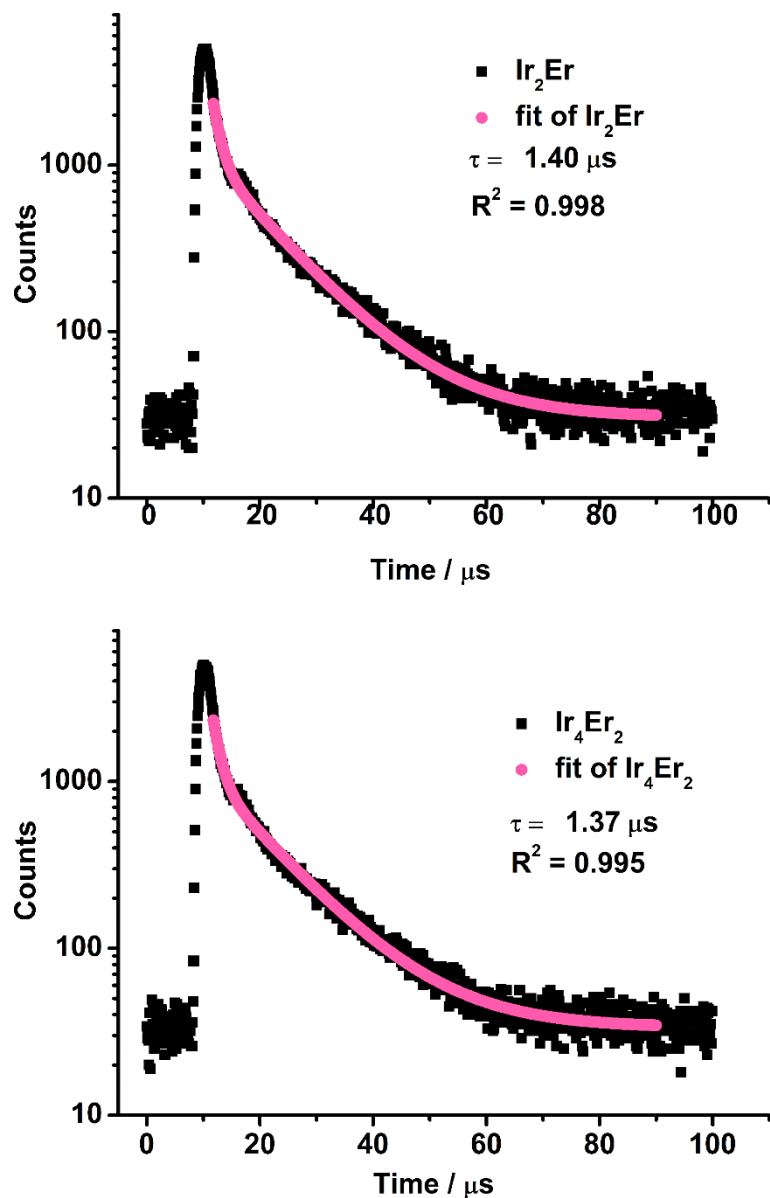


Figure S31. Luminescent decay profiles monitored at 1538 nm for Ir_2Er and Ir_4Er_2 in the solid state at room temperature. The lifetime was fitted by bi-exponential function $I = A + B_1\exp(-t/\tau_1) + B_2\exp(-t/\tau_2)$.

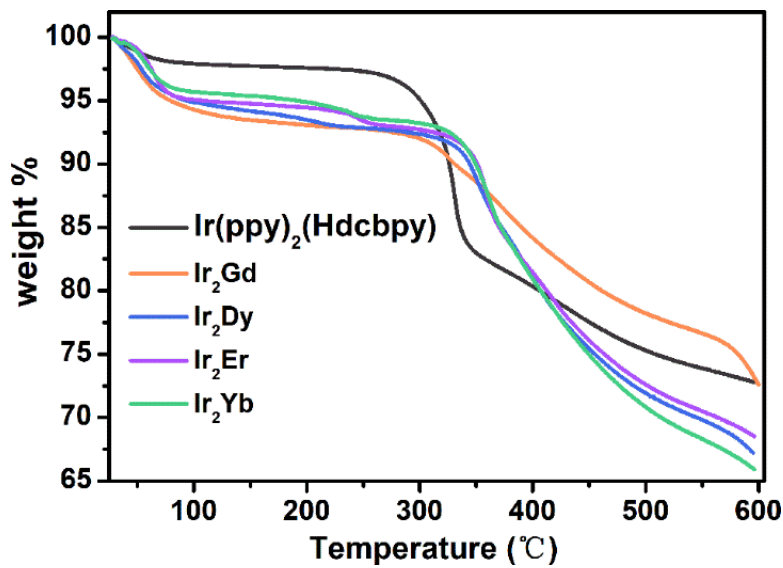


Figure S32. TGA curve of Ir_2Ln and $\text{Ir}(\text{ppy})_2(\text{Hdcbpy})$.

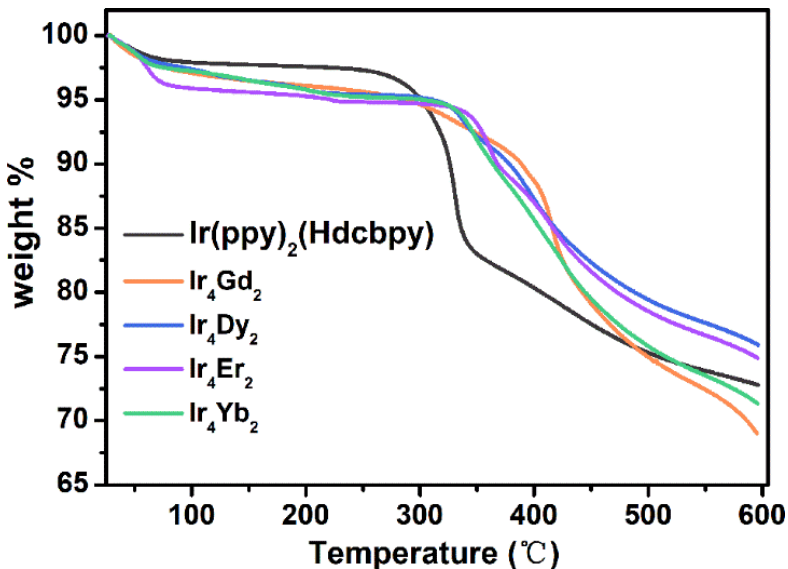


Figure S33. TGA curve of Ir_4Ln_2 and $\text{Ir}(\text{ppy})_2(\text{Hdcbpy})$.